forests

MDPI

Article

Effects of Burn Severity and Environmental Conditions on Post-Fire Regeneration in Siberian Larch Forest

Thuan Chu [1,2,*], Xulin Guo [1] and Kazuo Takeda [3]

[1] Department of Geography and Planning, University of Saskatchewan, Saskatoon, SK S7N5C8, Canada; xulin.guo@usask.ca
[2] Department of Forest Inventory and Planning, Vietnam Forestry University, Chuong My, Ha Noi 100000, Vietnam
[3] Department of Agro-Environmental Science, Obihiro University of Agriculture and Veterinary Medicine, Hokkaido 080-0834, Japan; takeda3@obihiro.ac.jp
* Correspondence: thuan.chu@usask.ca; Tel.: +1-306-966-5663

Academic Editors: Sean P. Healey and Warren B. Cohen
Received: 11 January 2017; Accepted: 7 March 2017; Published: 11 March 2017

Abstract: Post-fire forest regeneration is strongly influenced by abiotic and biotic heterogeneity in the pre- and post-fire environments, including fire regimes, species characteristics, landforms, hydrology, regional climate, and soil properties. Assessing these drivers is key to understanding the long-term effects of fire disturbances on forest succession. We evaluated multiple factors influencing patterns of variability in a post-fire boreal Larch (*Larix sibirica*) forest in Siberia. A time-series of remote sensing images was analyzed to estimate post-fire recovery as a response variable across the burned area in 1996. Our results suggested that burn severity and water content were primary controllers of both Larch forest recruitment and green vegetation cover as defined by the forest recovery index (FRI) and the fractional vegetation cover (FVC), respectively. We found a high rate of Larch forest recruitment in sites of moderate burn severity, while a more severe burn was the preferable condition for quick occupation by vegetation that included early seral communities of shrubs, grasses, conifers and broadleaf trees. Sites close to water and that received higher solar energy during the summer months showed a higher rate of both recovery types, defined by the FRI and FVC, dependent on burn severity. In addition to these factors, topographic variables and pre-fire condition were important predictors of post-fire forest patterns. These results have direct implications for the post-fire forest management in the Siberian boreal Larch region.

Keywords: post-fire regeneration; forest recruitment; vegetation recovery; *Larix sibirica*; remote sensing; Siberia

1. Introduction

Larix sibirica Ledeb. (Siberian Larch) is the dominant tree species covering approximately 80% of forests in the southern limit of the Siberian taiga of northern Mongolia. This Larch forest in the taiga forest-steppe transition zone is particularly vulnerable to climate change and fire disturbance [1,2]. Coupled with a growing demand for wood products and environmental services, increasing rates of natural disturbances such as fire and climate change has highlighted technical and scientific gaps in managing for the persistence of the Siberian Larch forest [3]. An improved understanding of the biogeochemical and biogeophysical properties and mechanisms that determine patterns in the post-disturbance Larch forest is thus a key step to manage the forest sustainably.

Several field-based studies have demonstrated that composition and growth of the boreal Larch forests are influenced by fire and climate change [1–4]. Otoda et al. [2] found that regeneration patterns

after fire vary by tree species. *Betula platyphylla* Sukaczev. (Asian White Birch) regenerates vigorously after fire and is not dependent on seed sources. This contrasts with the post-fire regeneration of Siberian Larch that is dependent on the presence of nearby seed sources. Similar to *Picea mariana* (Black Spruce) in the North American boreal forest, high fire frequency and large burned areas in the boreal Siberian Larch forest are likely to promote the relative dominance of broadleaf trees and threaten the persistence of coniferous species [2,5,6].

In addition to biotic factors, burn severity is one of the most important abiotic disturbance attributes that shape variation in post-fire regeneration [7]. Cai et al. [8] found that regenerated densities of Siberian Larch and Birch after a fire are both inversely related to burn severity. This is similar to the North American boreal forest where higher burn severity results in lower stem density and biomass of Black Spruce [6]. Other abiotic and biotic factors such as post-fire understory cover, soil moisture, soil organic depth and topography (i.e., elevation, slope, aspect) have less influence on post-fire forest patterns [8–10]. As well, climate trends underlie remarkable regional variation in the boreal Larch forest regrowth even within the same mountain system [1]. From tree-ring analysis, Dulamsuren et al. [1,4,11] found that annual tree-ring growth of Siberian Larch is negatively correlated with summer temperature while it has a positive relationship with the summer precipitation.

Despite the relevance of multiple fire and environmental factors for tree regeneration in the Siberian Larch forest, few studies have assessed the integrated influence of these factors at a relevant, landscape level. This lack of information has led to uncertainty in predicting important responses of the Siberian Larch forest to disturbance, particularly in the taiga-steppe transition zone. Remote sensing with its abundant data sources and time efficiencies offers considerable potential not only for tracking forest patterns but also for evaluating driving factors of forest regeneration after fire. Compared to field-based methods, remote sensing approaches enable forest researchers and managers to model the influence of key drivers on the post-fire forest patterns within a larger, landscape scale, spatial context.

Vegetation indices, such as Normalized Difference Vegetation Index (NDVI) and Enhanced Vegetation Index (EVI) have been the most frequently used response variables representing the composition and structure of post-fire forest [12–15]. The assumption that variation in these vegetation indices equates to forest recovery may be inappropriate and remains uncertain due to multiple layers of vegetation and substrate in the post-fire environment [16–18].

Similar to the Spectral Mixture Analysis (SMA) [18], the Fractional Vegetation Cover (FVC), a continuous scale of the areal proportion of the landscape occupied by green vegetation [19], is a promising index for evaluating post-fire vegetation regrowth [20]. Additionally, the integrated forest z-score (IFZ) [21] indicates the probability that a non-forest pixel will become a forest pixel. This can also be an indicator of the post-fire forest recovery [22]. In our recent study [23], the Landsat time-series of the FVC and the IFZ based Forest Recovery Index (FRI) have both been shown to successfully capture different pathways of post-fire forest recovery in the Siberian Larch forest. The FVC Landsat time-series can represent the early stages of the boreal Larch forest succession that dramatically quickens pace 5–6 years after the fire. Alternatively, the FRI time-series is more suitable to observe the regrowth of the Larch forest at later successional stages (e.g., the tenth year after the fire) [23]. In this study, we further assessed the effects of the burn severity and environmental conditions on post-fire forest patterns by using the FVC and FRI as response variables during different stages of Larch forest succession. More specifically, our objectives are (1) to evaluate the influence of a selected set of environmental factors on the variability of the post-fire forest recovery rate at different stages of the forest succession; and (2) to examine the degree of interaction among these driving factors in determining the forest recovery pattern after fire disturbances. Throughout this study, the term green vegetation recovery refers to the regrowth of all vegetation types following fire (i.e., herbaceous plants, shrubs, grasses, broadleaf and conifer trees) while the term forest regeneration, more specifically, refers to the regeneration of dominant Larch trees in the post-fire environment. This study provides an example of the primary use of the remotely sensed data for evaluating post-fire

forest regeneration in which different successional pathways have been considered. Our results present an opportunity for forest managers to develop methods to rapidly evaluate as well as continuously monitor vegetation responses after the fire disturbances, particularly in the vast, remote regions of the Siberian boreal forest.

2. Materials and Methods

2.1. Study Area

Our study was conducted in the boreal Larch forest of Hovsgol province, northern Mongolia (49°38′ N, 100°10′ E) (Figure 1). The Siberian Larch (*Larix sibirica*) is a dominant species in the forest composition of the study area followed by *Pinus sibirica* Du Tour (Siberian Pine), *Pinus sylvestrus* L. (Scots Pine), *Picea obovata* Ledeb. (Siberian Spruce), *Betula platyphylla* Sukaczev. (Asian White Birch), *Salix spp.* (willow), *Populus tremula* L. (Trembling Aspen), and *Ulmus pumila* L. (Siberian Elm) [3,24]. In contrast to other coniferous ecosystems, Larch dominated forest is deciduous with unique ecological characteristics and successional patterns that usually do not include an early stage of dominance by broadleaf species [25]. The area has been recently heavily affected by severe fires caused by both human and lighting sources [26,27]. Our study focused on a large wildfire area in June 1996 [28] that affected approximately 280 km^2 of predominantly Siberian Larch forest. The same burned area and detailed descriptions of the northern Mongolia ecosystem can be found in Chu et al. [23,29].

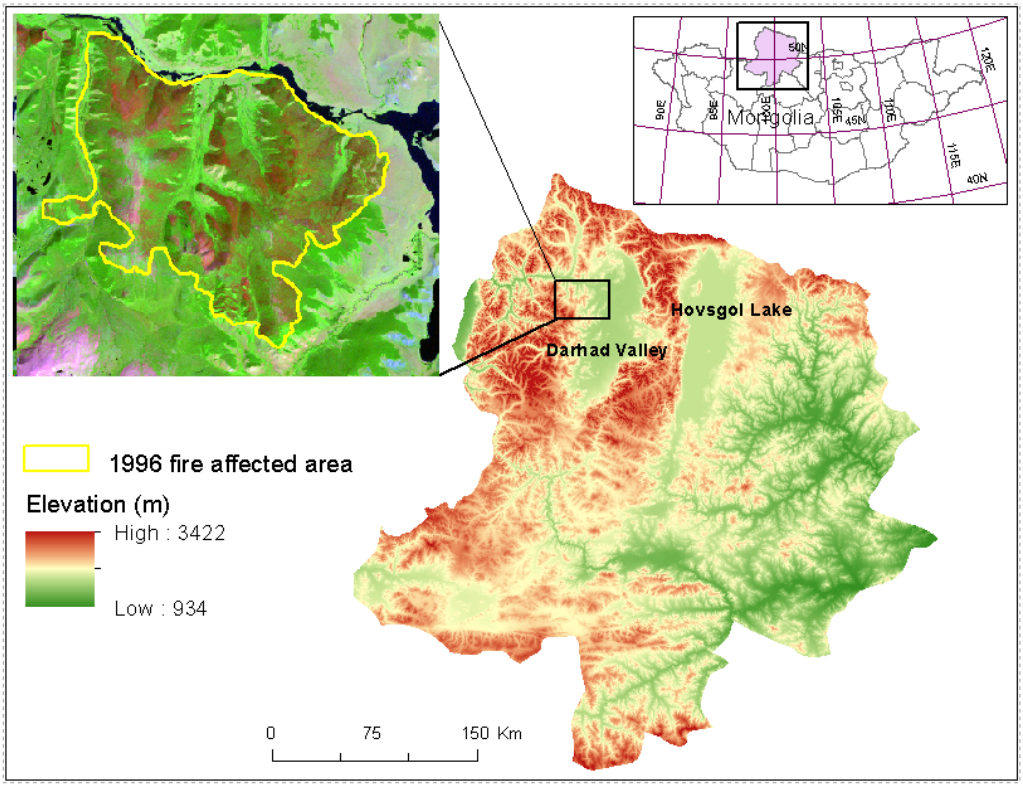

Figure 1. The study area. The 1996 fire affected area (top left corner) was overlaid on the 1998 Landsat TM image (R:G:B = 7:4:1).

2.2. Datasets and Preprocessing

We used Landsat datasets as reported in Chu et al. [23]. In summary, the data comprised nine Landsat TM, six Landsat ETM+, and one Landsat OLI scenes in the same path of 137 and row of 24 (Table 1). All images were selected during peak-summer months (July and August) to minimize the

influence of atmospheric conditions and vegetation phenology difference on estimates of time-series forest regrowth. All available images were downloaded from the USGS (United States Geological Survey) website [30].

Table 1. Time-series Landsat images for assessing drivers of post-fire Larch forest patterns in the 1996 burned area in northern Mongolia. No images in 1997, 2006, and 2012 were found for the study area.

ID	Acquisition Date	Sensor	Year Since Fire (YSF)
1	30/6/1995	TM	Pre-fire
2	25/8/1998	TM	2
3	5/9/1999	ETM+	3
4	29/7/2000	TM	4
5	16/7/2001	TM	5
6	19/7/2002	TM	6
7	6/7/2003	TM	7
8	16/7/2004	ETM+	8
9	4/8/2005	ETM+	9
10	9/7/2007	ETM+	11
11	12/8/2008	ETM+	12
12	6/7/2009	TM	13
13	25/7/2010	TM	14
14	12/7/2011	TM	15
15	3/9/2013	OLI	17
16	12/7/2014	ETM+	18

We processed the data using atmospheric and topographic corrections (Chu et al. [23]). The relative geometric correction was applied to our Landsat time-series data in which all images in the time-series were geo-corrected relative to a 1995 master. This step enhances the spatial accuracy of the image time-series (i.e., FVC and FRI), improving temporal change detection of the post-fire forest. In the correction of atmospheric condition, we selected the relative method of "absolute-normalization" [31,32]. Absolute-normalization atmospheric correction matches all images in a time-series to an atmospherically corrected reference image [31]. We first applied the absolute atmospheric correction of surface reflectance on the 1998 reference image using the ATCOR (Atmospheric and Topographic Correction) algorithm [33]. All remaining images in the Landsat time series were then normalized to the corrected 1998 image using the iteratively re-weighted MAD (multivariate alteration detection) algorithms of Canty and Nielsen [32].

In addition to Landsat data, a 90-m grid, digital elevation model from the Shuttle Radar Topography Mission (SRTM; [34]) for the study area was acquired. We resampled it to 30 m grid size for calculation of topographic variables (e.g., slope and solar radiation) and satellite image correction.

The field survey was conducted from 2007 to 2009 at two different locations of the 1996 and 1991 burned areas [23] (see Section 2.3.2 in [23] for more detail). Within the location of each burned area, the data related to post-fire forest patterns such as biophysical parameters of unburned adult trees, seedlings and saplings were collected. Due to the limited access to the field, the distribution and number of field samples were insufficient to evaluate quantitatively the results from remotely sensed observation. It should be noted that the pre-fire condition of both burned areas was similar. Therefore, all field data, surveyed on the 1996 and 1991 burned areas, were summarized at different burn severity for the comparative analysis of the model accuracy in this study.

2.3. Indicators of Vegetation Response after Fire

Chu et al. [23] demonstrated that the FVC method can be used to monitor the regrowth of the green vegetation cover in an early stage of the forest succession. They also showed that the FRI method is useful to represent Larch forest regeneration in later stages of post-fire forest succession. The use of both FVC and FRI as response variables in this study was expected to account for different pathways

of post-fire Larch forest succession that are driven by burn severity and environmental conditions in the taiga-steppe transition zone.

The time series of FVC and FRI were calculated based on Landsat time series data and the interpretation of high resolution WorldView-2 images and field data [23]. An NDVI based technique was used to calculate the FVC [19,35–37] in which pixels were scaled between bare soil ($NDVI_s$) and dense vegetation index ($NDVI_v$) values (Equation (1)):

$$FVC = \frac{NDVI - NDVI_s}{NDVI_v - NDVI_s} \quad (1)$$

where NDVI is given by $NDVI = \frac{\rho_{nir} - \rho_{red}}{\rho_{nir} + \rho_{red}}$; ρ_{nir} and ρ_{red} are corrected reflectance obtained from sensor bands located in the near infrared (NIR) and red spectral regions for each pixel within an image [38]. $NDVI_s$ and $NDVI_v$ are values of NDVI for bare soil (FVC = 0) and pure green vegetation (FVC = 1) within an image, respectively. The FRI was proposed by Chu et al. [23] based on the integrated forest z-score (IFZ) of Huang et al. [21] (Equation (2)).

$$FRI = \frac{1}{IFZ} = \frac{1}{\sqrt{\frac{1}{NB}\sum_{i=1}^{NB}(FZ_i)^2}} \quad (2)$$

where IFZ is the integrated forest z-score [21] estimated from the forest z-score of each spectral band i: $FZ_i = \frac{b_{pi} - \overline{b_i}}{SD_i}$; $\overline{b_i}$ and SD_i are the mean and standard deviation of the band i spectral values of known forest samples, respectively; NB is number of bands used. For Landsat images, Red (630–690 nm), SWIR1—Short Wave Infrared 1 (1550–1750 nm), and SWIR2—Short Wave Infrared 2 (2080–2350 nm) are used to calculate the IFZ values [22]. Our temporal trajectory of FVC and FRI [23], using logistic and polynomial regressions, showed that the FVC increases dramatically after the fire disturbances while FRI, possibly showing both the post-fire tree mortality and the Larch regeneration, decreases for the first 10 years after fire and then gradually increases (Figure 2). Our previous study [23] shows that the increasing trend of FVC and FRI is equivalent to the progress of green vegetation recovery and Larch forest regeneration following fire, respectively. Additionally, we focused on how the Larch forest and other species recover spatiotemporally after fire. Therefore, the only periods showing an increasing trend of FVC and FRI were selected to establish least squares relationship using Equations (3) and (4):

$$fFVC = \beta_{FVC} \times YSF + \beta_{1\times} \quad (3)$$

and

$$fFRI = \beta_{FRI} \times YSF + \beta_2 \quad (4)$$

where the fFVC and the fFRI are the annual growth of green vegetation cover and Larch forest recruitment of each post-fire year to the pre-fire level, and YSF is the number of years since the fire. The β_{FVC} and β_{FRI} were the slope of the post-fire trend of the FVC and FRI and are defined as the rates of vegetation recovery and Larch forest regeneration of the post-fire forest, respectively.

The temporal patterns of FVC and FRI (i.e., Equations (3) and (4)) were applied on a per pixel basis to derive the spatiotemporal patterns of the forest recovery, using pixel-wise least squares regression. Only the time-period showing an increasing trend in the temporal trajectory of the forest recovery was selected for the analysis of spatiotemporal forest patterns. Consequently, all cloud-free FVC images from 1998 to 2014 (i.e., YSF 2 to 18) were used to estimate the rate of vegetation recovery while cloud-free FRI images from 2007 to 2014 (i.e., YSF 11 to 18) were used to capture an increasing trend of FRI values illustrating the Larch forest recruitment after fire. The results of spatiotemporal patterns of forest recovery based on the slope of the post-fire trend of the FVC and FRI (i.e., β_{FVC} and β_{FRI}) for the burned area in 1996 are shown in Figure 3 (Adapted from [23]). Positive slopes for FVC and FRI represent an increasing trend of forest cover while negative slopes indicate the decreasing trend of forest cover. The p-value from linear regressions revealed whether recovery was statistically significant.

The continuous values of both FVC and FRI slopes (i.e., β_{FVC} and β_{FRI}) were used as the response variables for modeling post-fire forest patterns. Hereafter, we will use the terms green vegetation recovery rate (i.e., grasses, shrubs and broadleaf trees dominated regrowth) and forest recovery rate (i.e., Larch dominated regrowth) to refer to the annual post-fire change in the FVC and the FRI slopes (β_{FVC} and β_{FRI}), respectively as the analysis results of the FVC and FRI time series and the least squares regressions on a per pixel basis (Figure 3).

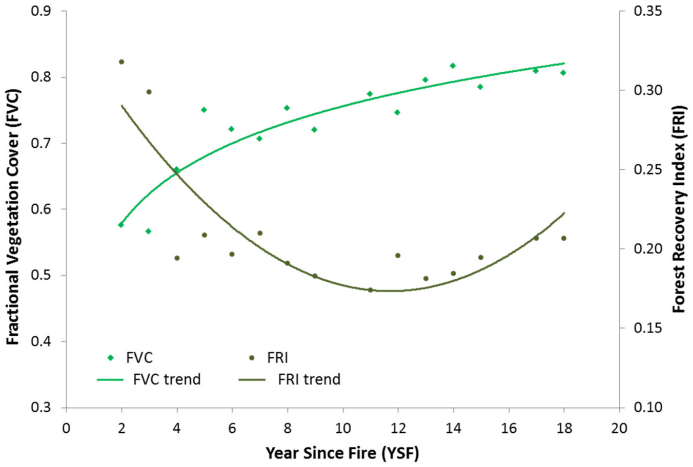

Figure 2. Temporal trend of post-fire forest patterns measured by FVC (Fractional Vegetation Cover) and FRI (Forest Recovery Index) from Landsat time series data. The trends were fitted using the logistic and polynomial regressions based on the annual mean values of FVC and FRI and the year since fire (YSF), respectively (see [23]). Only the periods showing an increasing trend of the FVC and FRI were selected to calculate the forest recovery rate after fire using the Equations (3) and (4).

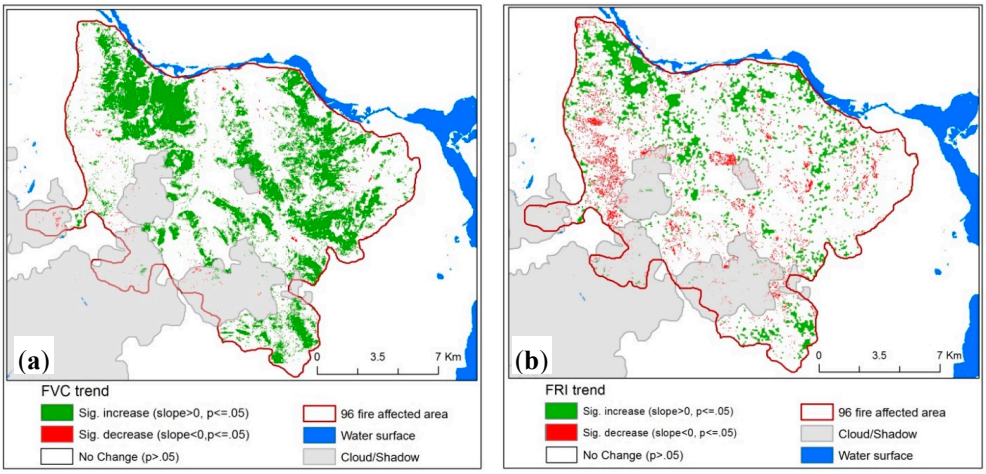

Figure 3. Post-fire Larch forest patterns estimated using FVC slope and its p-value, an indicator of occupation rate of post-fire vegetation cover—early successional stage (**a**); and the slope of the FRI trend and its p-value, an indicator of Larch forest recruitment—later successional stage (**b**). The continuous values of both FVC and FRI slopes were extracted and used as response variables in modeling post-fire forest patterns.

2.4. Exploring Drivers of Post-Fire Forest Pattern

Eight explanatory environmental variables from the Landsat imagery and other data sources were derived to model post-fire forest patterns. These variables were grouped into three categories: pre- and post-fire forest condition; local landscape; and topographic condition (Table 2).

Table 2. Fire disturbance attributes and environmental factors as potential predictors of post-fire forest pattern.

Variable Group	Indicator	Description	Unit/Variable Type	Source
		Response variables		
Post-fire forest pattern/forest recovery rate	Fractional vegetation cover (FVC)	FVC determines the proportion of burned land surface occupied by vegetation recovery. It not only represents Larch forest recruitment but also the early seral community of shrubs, grasses, and broadleaf trees. Post-fire slopes of the fitted FVC by year since fire were used as the rate of post-fire vegetation recovery in early seral vegetation.	Continuous	Analysis of post-fire Landsat time series FVC data (1998–2014) [23]
	Forest recovery index (FRI)	FRI estimates whether a disturbed Larch forest pixel is recovering to a Larch forest pixel. Post-fire slopes of the fitted FRI by year since fire were used as the rate of post-fire forest recruitment.	Continuous	Analysis of post-fire Landsat time series FRI data (1998–2014) [23]
		Explanatory variables		
Pre- and post-fire forest condition	Pre-fire forest NDVI	The Normalized Vegetation Difference Index (NDVI) is a common indicator to evaluate forest health including tree density, tree age, and basal area. These pre-fire properties have a strong effect on post-fire forest regeneration. The pre-fire NDVI within Larch forest locations was thus selected as an indicator of pre-fire forest condition.	Continuous (0 ÷ 1)	Derived from red and near infrared band of the pre-fire 1995 Landsat image
	Burn severity	The burn severity is defined as the degree of ecosystem change attributed to fire disturbance. Three burn levels (low, moderate and high severity) were derived from our burn severity model of the study area.	Categorical with value of 1 (low), 2 (moderate) and 3 (high) severity	Burn severity model for the Siberian boreal Larch forest [29]
	Post-fire vegetation and soil moisture	The temperature–vegetation dryness index TVDI is a remote sensing based index that provides an indication of drought condition. The TVDI is negatively related to vegetation and soil water content. Higher TVDI results from the combination of lower precipitation and higher evaporation rate. This study used an 18-year mean of post-fire TVDI as indicator of post-fire vegetation and soil moisture condition.	Continuous (0 ÷ 1)	Derived from the relationship between surface temperature (T_s) and NDVI that were extracted from Landsat time series (1998–2014)
Topographic variables	Solar insolation	The Solar insolation or solar radiation is the total amount of solar energy received at a particular location during a specified time period. It is an indicator of photosynthetically active radiation, soil moisture and soil temperature. The total amount of solar insolation in each location within the burned area was averaged during summer months in the study area.	Continuous (MWH/m^2)	Derived from a digital elevation model (DEM)
	Elevation	The elevation within each pixel. Shuttle Radar Topography Mission (SRTM) digital elevation was interpolated and resampled to 30 m resolution.	Continuous (m)	SRTM digital elevation model
	Slope	The slope within each pixel location of the burned area that was derived from DEM.	Continuous (deg.)	Digital elevation model
Local landscape	Distance to water body/Hydrology	The distance to the water surface is an indicator of water content in the air and soil environment. Higher soil moisture and cooler air can be found near the water surface. It was calculated by Euclidean distance to water body that masked from the satellite imagery.	Continuous (km)	Analysis of Euclidean distance and masked water surface from Landsat imagery
	Land cover types	Pre-fire land cover types may indicate the potential for forest recovery due to post-fire seed availability and soil condition. The pre-fire land cover types of Larch forest and non-Larch forest were evaluated to compare the recovery rate between these cover types.	Categorical with value of 1 (Larch forest) and 0 (other vegetation)	Classification of pre-fire land covers type based on forest z-score (IFZ) from Landsat images [23]

2.4.1. Pre- and Post-Fire Forest Condition

Pre-fire vegetation condition (i.e., tree density, tree age, basal area, biomass, and species composition) may influence post-fire forest regeneration due to its relationship with the post-fire burn severity, the seed availability and the seed germination [9,39–45]. Since NDVI is the most common remote sensing index and has shown consistent correlation with the vegetation condition and biophysical parameters [46], we used it to represent the pre-fire vegetation condition. Within the burned Larch forest area, higher pre-fire NDVI was expected to correlate positively with forest conditions that provide a suitable post-fire environment for seedling and sapling recruitment.

Regarding the fire regime, fire frequency, fire intensity, and fire and burn severity are important factors that alter post-fire forest composition and structure [12]. Fire severity is the degree of environmental change caused directly by fire assessing immediately after a fire event (i.e., an initial assessment), while burn severity is defined as fire-induced changes in vegetation cover and assessed by a certain amount of time elapsed after a fire (i.e., an extended assessment) [7,12,47]. As the satellite imagery was not available immediately after the fire event to assess fire severity, the term "burn severity" is used throughout this study to evaluate the influence of fire behavior on post-fire forest patterns. Using the differenced Normalized Burn Ratio (dNBR) [48] and classification and regression tree (CART) model, Chu et al. [29] conducted the assessment of burn severity in the same study area in northern Mongolia. The dNBR values ($dNBR = NBR_{pre\text{-}fire} - NBR_{post\text{-}fire}$). NBR was calculated using the equation (NIR-SWIR2)/(NIR+SWIR2), where the NIR and the SWIR2 are near infrared and short wave infrared Landsat bands respectively. We then scaled NBR by 1000 and classified it into four bins of high severity ($dNBR \geq 440$), moderate severity ($190 \leq dNBR < 440$), low severity ($70 \leq dNBR < 190$), and unburned ($dNBR < 70$). The Landsat images acquired in 1995 and 1998 were used as pre- and post-fire images, respectively, for the calculation of the dNBR. Readers are referred to Chu et al. [29] for details of the methodology and results in mapping burn severity for the Siberian larch forest.

Many studies have shown that surface soil temperature and moisture determined by the organic layer depth after fire significantly controls the patterns of secondary succession in the boreal forest [45,49–51]. In remote sensing applications, the combination of NDVI and land surface temperature (T_s) can provide information on vegetation and soil moisture conditions. Sandholt et al. [52] suggested a water stress index called the temperature–vegetation dryness index (TVDI) based on analysis of a simplified triangular shape of NDVI-T_s space (Equation (5)). This index has been widely used in agricultural and forest meteorology to estimate soil moisture [52–56]. We used the TVDI as an indicator of soil moisture condition in the post-fire environment.

$$\text{TVDI} = \frac{T_s - T_{smin}}{T_{smax} - T_{smin}} \quad (5)$$

where T_s is the observed surface temperature at a given pixel; T_{smin} and T_{smax} are the minimum and maximum surface temperature, respectively, observed for a given NDVI. T_{smin} and T_{smax} are also defined as "wet edge" and "dry edge", respectively, in the triangle shape of NDVI-T_s space that can be modeled as linear fits to NDVI data (Equations (6) and (7)) [53,54,57,58]:

$$T_{smax} = a_1 + b_1(\text{NDVI}) \quad (6)$$

$$T_{smin} = a_2 + b_2(\text{NDVI}) \quad (7)$$

where a_1 and b_1 are parameters defining the dry edge; a_2 and b_2 are parameters defining the wet edge. These parameters are estimated on the basis of pixels from an area large enough to represent the entire range of surface moisture contents. The TVDI has been demonstrated to be negatively correlated with soil moisture, particularly at soil depths from 0 to 10 cm [53,54,56,59]. The value of the TVDI ranges from 1, indicating limited soil moisture availability to 0 representing unlimited water access and maximum evapotranspiration. Here, we derived the land surface temperature (T_s) from the thermal

band (10.4–12.5 μm) of the Landsat data using the ATCOR algorithm in Geomatica software (2013, PCI Geomatics, Markham, ON, Canada). We used an NDVI interval of 0.01 to estimate maximum and minimum T_S for regressing the dry and wet edge parameters, respectively. The time series of post-fire TVDI between 1998 and 2014 was used to calculate the post-fire mean TVDI as one of the explanatory variables of spatiotemporal vegetation recovery.

2.4.2. Topographic Variables

Topography is a significant factor related to the water availability, soil erosion, energy exchange and wind exposure that has a direct or indirect influence on the response of vegetation after fire [60,61]. In the boreal Larch forest, conifer species tend to regenerate faster in low-lying sites with a shallow slope, mesic flat and thick soil [8,62]. Upland and steep slope areas with moderate soil moisture content are ideal conditions for the broadleaf tree recruitment [8]. In our study, elevation, slope, and solar insolation were considered as a proxy for site conditions as well as indicators of the spatial arrangement of vegetation cover.

Incoming solar radiation (or solar insolation) is defined as the total amount of solar energy intercepted at a particular location during a specified time period. It is fundamental to most physical and biophysical processes because of its influence on the energy and water balance at the land surface, air and soil heating, evapotranspiration and photosynthesis of terrestrial ecosystems [63]. Photosynthetically active radiation that vegetation is able to use in the process of photosynthesis has a linear relationship with the solar insolation [64,65]. Therefore, solar insolation can be used as an indicator of the photosynthetically active radiation. Solar insolation varies significantly depending on elevation, surface orientation (slope and aspect), and obstruction by surrounding topographic features. Several studies used aspect to represent solar radiation in studies of biophysical processes including the forest regeneration [3,66]. However, using aspect to represent solar radiation may limit the interpretation of the vegetation dynamics driven by solar energy [67]. Here, we calculated the solar insolation using digital elevation model and a solar analyst model developed in ArcGIS by Fu and Rich [68]. We calculated the total solar insolation during each summer month—growing season (June–August) in the post-fire years—and averaged it to represent the mean solar insolation of the post-fire summer months. The mean solar insolation was used as an indicator of the regrowth variability within the burned area.

2.4.3. Local Landscape Variables

Landscape variables such as land cover type, landscape heterogeneity, and water surface have a significant effect not only on forest growth but also forest regeneration after disturbances [6,43,62,69,70]. Zhao et al. [62] found that the post-fire seed dispersal in Birch and Larch is higher than in Siberian Dwarf Pine (*Pinus pumila*). As a result, more Birch and Larch seedlings are found in burned areas than seedlings of Siberian Dwarf Pine [62]. In our study, the pre-fire Larch dominated forest was separated from other vegetation using the integrated forest z-score (IFZ) and the pre-fire 1995 image [23]. Larch forest regeneration was expected to proceed at a faster rate in the Larch burned area compared with the non-Larch burned area. Finally, because the study area is close to the water surface, including rivers and lakes (Figure 1), we used the distance to water body as an explanatory variable that can influence water content in the air and soil of the study area. Water body was extracted from the Landsat NDVI image and then the Euclidean distance to it was calculated and used as a predictor of forest recovery.

2.5. Modeling Post-Fire Forest Pattern

The Random Forest (RF) algorithm [71] in the R package ModelMap [72] was used to model the post-fire vegetation recovery rate (β_{FVC}) and the Larch recovery rate (β_{FRI}) as a function of driving factors (Table 2). The RF model is an extension of the non-parametric classification and regression trees (CART). The RF algorithm develops "forest" from the CART trees. For each CART model,

a random portion of the data are selected to train the model and the remaining data are used for the model validation. A random subset of the predictors is selected at each node split to ensure that the effects of all the predictors are tested. There are several advantages of RF over the traditional classification techniques: (1) through a bootstrap approach, it can obtain higher accuracies than the single classification tree methods; (2) it develops accurate and unbiased predictions based on selections across bootstrap replicates; (3) it is non-parametric and thus unaffected by the distributional assumptions [71,73].

The training and testing samples for the RF algorithm in this study were randomly selected from a set of raster layers of both response and predictor variables. In an attempt to keep the samples equal and fully randomized among the categorical predictor variables (e.g., burn severity and pre-fire forest classes), we used a stratified random design to generate approximately 450 samples for each burn severity class (i.e., low, moderate and high severity classes). These samples were equally located in both the burned Larch forest and burned non-Larch forest. For each sample location, both responses (e.g., slope values of the FVC and the FRI recovery trend) and predictor variables (pre-fire forest NDVI, burn severity, distance to water body, land cover types, solar radiation, elevation, and slope) were extracted on a per pixel basis using the bilinear interpolation method. Consequently, there were a total of 1350 samples with 70% of them used as a training dataset and 30% used for validation. Similar to other stochastic techniques, the RF model may introduce uncertainty to the final predictions since model runs can include highly correlated variables and results in spurious variation [74,75]. To reduce model uncertainty, multicollinearity among predictors was first examined using a variance inflation factor (VIF). All correlated factors were removed when the VIF exceeded the threshold value of 5 [76]. All proposed predictor variables (Table 2) were independent and thus included in the RF model. Second, the process of RF model tuning [74] was applied to the 70% training samples where the ntrees (i.e., number of trees) parameter in the model was selected based on building different RF models with increasing numbers of trees ranging from 100 to 2000 in 100 tree increments. Based on the 30% testing dataset, the numbers of trees that stabilized the role of predictor variables in determining response variables was then selected as an optimal ntrees parameter in the final RF model. Our analysis indicated that the importance of predictor variables to determine recovery rates stabilized between 1200 and 1650 trees, and thus a value of 1200 for ntrees was selected to reduce the processing time and computational complexity.

We report variance for each model as well as the importance of each predictor to the variance explained by the models. The variance explained for each model is similar to the coefficient of determination (R^2) for linear regressions that reports statistical fit to a given dataset. The independent validation dataset of the response and explanatory variables (i.e., 30% of the samples) was used to explain random forest variance. To measure the importance of the predictors, the RF algorithm randomly excludes the values for a single predictor with the remaining data used to predict the RF model across all trees. The resulting change in the mean square error from the original data was recorded and used as the variable importance measure. In addition, the interaction between predictor variables in explaining the response variable was also reported using three-dimensional interaction plots, in which two specified predictor variables are plotted on the x- and y-axis to determine the response variable plotted on z-axis [72,74]. Two sets of RF models were run in this study. In the first set, we examined how burn severity and environmental factors influence the vegetation recovery rate defined by the FVC method. In the second set, the forest recovery rate defined by the FRI method was evaluated. We expected that the degree of influence of the predictor variables on the vegetation recovery rate is different from that of the forest recovery rate since each response variable accounts for a different stage of the post-fire forest recovery. The overall processing steps of modeling drivers of the post-fire forest regeneration are shown in Figure 4.

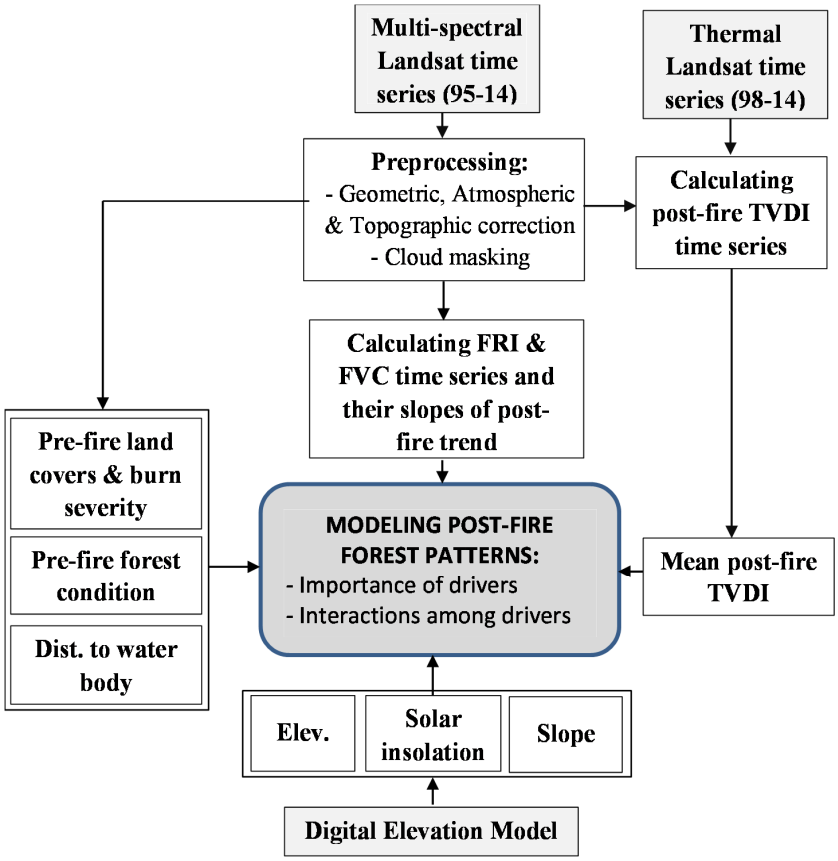

Figure 4. Overall processing flow of modeling drivers of the post-fire forest regeneration in the Siberian boreal Larch forest.

3. Results

3.1. Calculation of Drivers

3.1.1. Pre- and Post-Fire Vegetation Conditions

The 1995 Landsat TM was selected as the image to calculate the pre-fire NDVI (Figure 5). The zonal statistic showed that the area of significant increase in the post-fire FVC and FRI slope had higher values of pre-fire NDVI than the area of significant decrease in the FVC and FRI slope, 0.65 and 0.46 respectively. This highlights the importance of the pre-fire forest condition in the recovery of the forest after fire disturbances in which healthier pre-fire forest conditions determined by the higher NDVI value may result in a faster forest recovery rate.

The result of mapping burn severity based on the pre-fire (1995) Landsat image and the post-fire (1998) Landsat image is also shown in Figure 5. We found 59% of the area showed a significant increase in the FVC trend (or significant increase of vegetation cover) after fire in the moderate severity areas, while 26% and 15% of that area was located in the high and low severity burns. However, the rate of vegetation recovery was highest in the high burn severity area ($\beta_{FVCmean}$ = 0.04), followed by the moderate ($\beta_{FVCmean}$ = 0.024) and low burn severity areas ($\beta_{FVCmean}$ = 0.016). The results of Larch forest recovery showed that 45% of the area with a significant increase in FRI trend (i.e., significant increase of forest regeneration) after fire was in the moderate burn severity area, followed by the low (35%), and high (20%) severity burns areas. The moderate burn severity sites had the highest recovery rate as measured by the FRI slope ($\beta_{FRImean}$ = 0.01), followed by low ($\beta_{FRImean}$ = 0.006) and high ($\beta_{FRImean}$ = 0.003) burn severity sites.

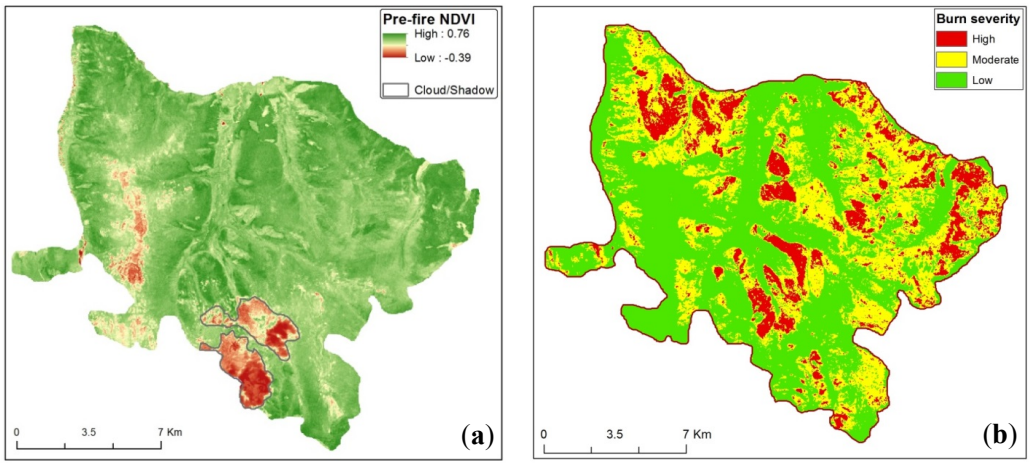

Figure 5. Pre-fire forest condition defined by the NDVI (**a**) and post-fire forest effects defined by burn severity (**b**). The burn severity classes were coded using categorical values of 1 for low, 2 for moderate, and 3 for high burn severity (Adapted from [29]).

To measure vegetation and soil water content in the post-fire environment, we calculated the 18-year mean TVDI during the post-fire years (1998–2014) from NDVI and land surface temperature (T_S) using NDVI-T_s space (Figure 6). As higher TVDI values indicate lower soil moisture, forest regeneration is expected to have an inverse relationship with TVDI.

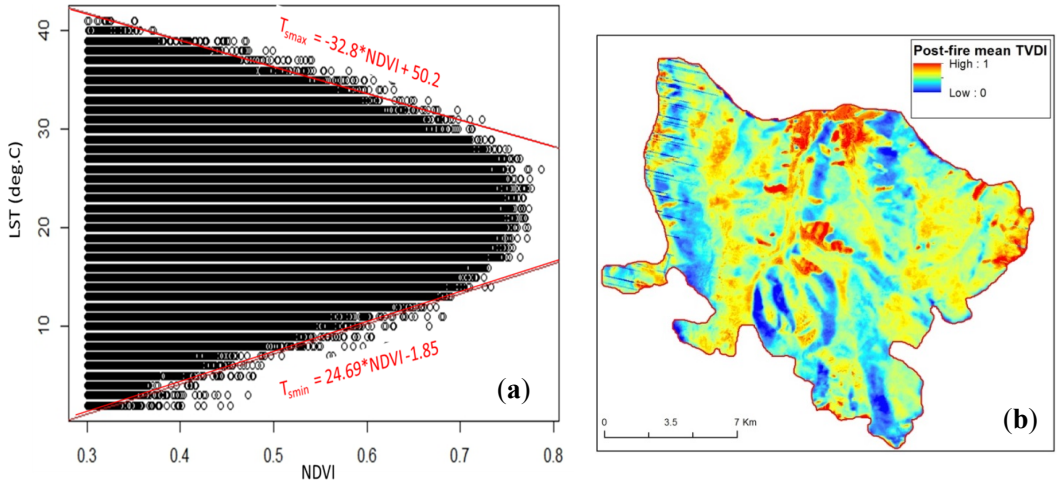

Figure 6. An example of the NDVI-T_s space and the determination of dry edge (T_{Smax} = −32.8 × NDVI + 50.2) and wet edge (T_{Smin} = 24.69 × NDVI − 1.85) for the calculation of the TVDI in 2000 (**a**) and the mean TVDI of the post-fire 18-years (1998–2014) (**b**). LST—Land Surface Temperature; TVDI—Temperature–Vegetation Dryness Index.

3.1.2. Topographic and Local Landscape Variables

Topographic values were derived from the SRTM digital elevation model (DEM) (Figure 7a,b). We found higher solar insolation in summer months in the south, southeast and southwest aspects that should result in the higher vegetation recovery rate. The slope predictor variable not only affects the amount of solar radiation striking the land surface, but also correlates to physical properties and constraints of soil (e.g., erosion, depth, moisture, and nutrients) for vegetation growth [77–79]. In the boreal Larch forest, it is expected that broadleaf tree recruitment is faster in upland sites with steep slopes compared with conifer recruitment [8].

Finally, two landscape variables (pre-fire land cover types and distance to water body) were measured for modeling post-fire forest patterns (Figure 7c,d). The results of zonal statistical analysis showed that there was a slight difference in the vegetation recovery rate measured by the FVC between the Larch burned forest and non-Larch burned forest with mean FVC slopes ($\beta_{FVCmean}$) of 0.024 and 0.023 respectively. However, the forest recovery rate measured by FRI in the Larch burned area was much higher than that in the non-Larch burn area (0.013 and 0.0001 respectively). This demonstrated the influence of pre-fire land cover on the post-fire tree recruitment. Furthermore, significantly, it confirmed our findings regarding the measurement of the post-fire vegetation and forest recovery using the FVC and FRI methods. The FVC method is suitable to measure all green vegetation recovery (e.g., herbaceous plants, grasses, shrubs, broadleaf and conifer trees), while the FRI method is suitable to estimate pre-fire tree recruitment (e.g., Larch trees).

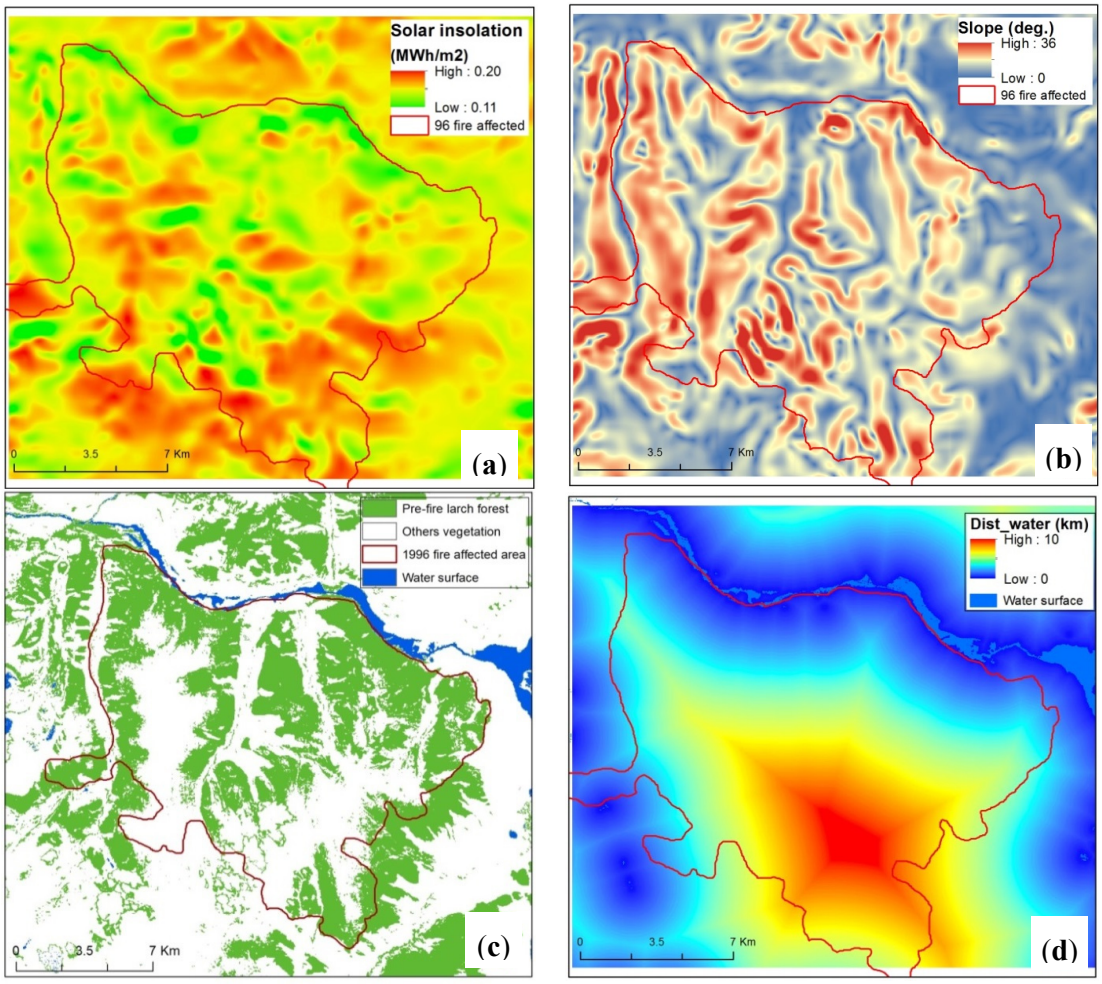

Figure 7. Examples of the topographic and landscape variables. Average solar insolation of summer months (**a**) and slope map (**b**) were derived from the surface analysis of a digital elevation model. Classification of pre-fire land covers using the 1995 integrated forest z-score (**c**) and the distance to water body using Euclidean distance (**d**). The water surface was masked using a 1995 NDVI Landsat image.

3.2. Modeling Post-Fire Forest Recovery

3.2.1. Modeling FVC Based Vegetation Recovery

Results from the random forest algorithm using a set of environmental predictors reveal that approximately 51% of the variation in the vegetation recovery rate measured by the FVC can be

explained by the predictor variables selected for this study (burn severity, elevation, distance to water, dryness temperature, solar insolation, pre-fire NDVI, slope and land cover type, Table 2). Model validation using an independent dataset also showed a good fit between the observed and predicted values of the vegetation recovery rate defined by the FVC slope. We found that burn severity was the most important factor explaining vegetation recovery, followed by elevation, water and solar energy related variables (Figure 8). Since the recovery of green vegetation in the post-fire environment includes not only Larch tree recruitment but also other early seral vegetation types, the pre-fire forest condition and land cover types that might determine seed source availability for Larch forest regeneration were less important than other variables in classifying the FVC based vegetation recovery rate.

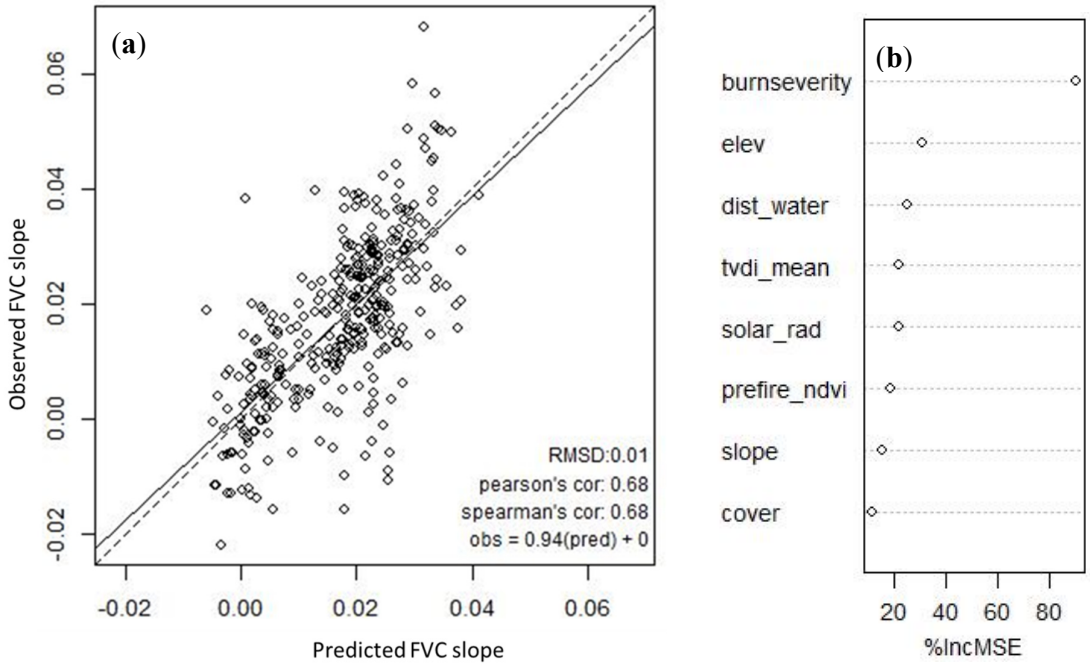

Figure 8. Observed and estimated FVC based vegetation recovery rate (or FVC slope) using the random forest algorithm (**a**) and the importance of predictors in classifying recovery rates (**b**). The dashed line is the 1:1 relationship and the solid line shows the linear best-fit between the observed and predicted vegetation recovery rate (the FVC slope) using the random forest (RF) algorithm. Variable importance measures the increase of mean square error (MSE) in the classification of the response variable if one predictor is excluded from the model.

The independent (or testing) samples were used to estimate the vegetation recovery rate plotted in the *z*-axis based on the interaction between two specified predictor variables plotted in the *x*- and *y*-axis (Figure 9). In this study, we observed the interaction of variable burn severity with other predictors in the determination of vegetation recovery. The remaining predictor variables were fixed at their mean (for continuous predictors) or their mode (for categorical predictors) in each interaction plot. The results showed that the FVC based vegetation recovery rate was positively correlated with burn severity, pre-fire vegetation condition, solar radiation, and slope (Figure 9d–f). Similar to the temporal trajectory of forest pattern in different burn severity classes [23], post-fire vegetation recovery measured by the FVC slope had the highest rate in high burn severity sites, followed by the moderate and low burn severity. The highest rate of vegetation recovery was also found in the altitude range from 1700 to 1900 m and that had burned with high severity (Figure 9a). Distance to water seems to negatively correlate with vegetation recovery where the highest recovery rate was found in the areas with high burn severity and within 2 km from the water body (Figure 9b). Even though the relationship between soil moisture measured by the TVDI and vegetation recovery rate was not clear,

areas with high burn severity likely recovered more quickly when they have higher soil moisture defined by lower TVDI values (Figure 9c).

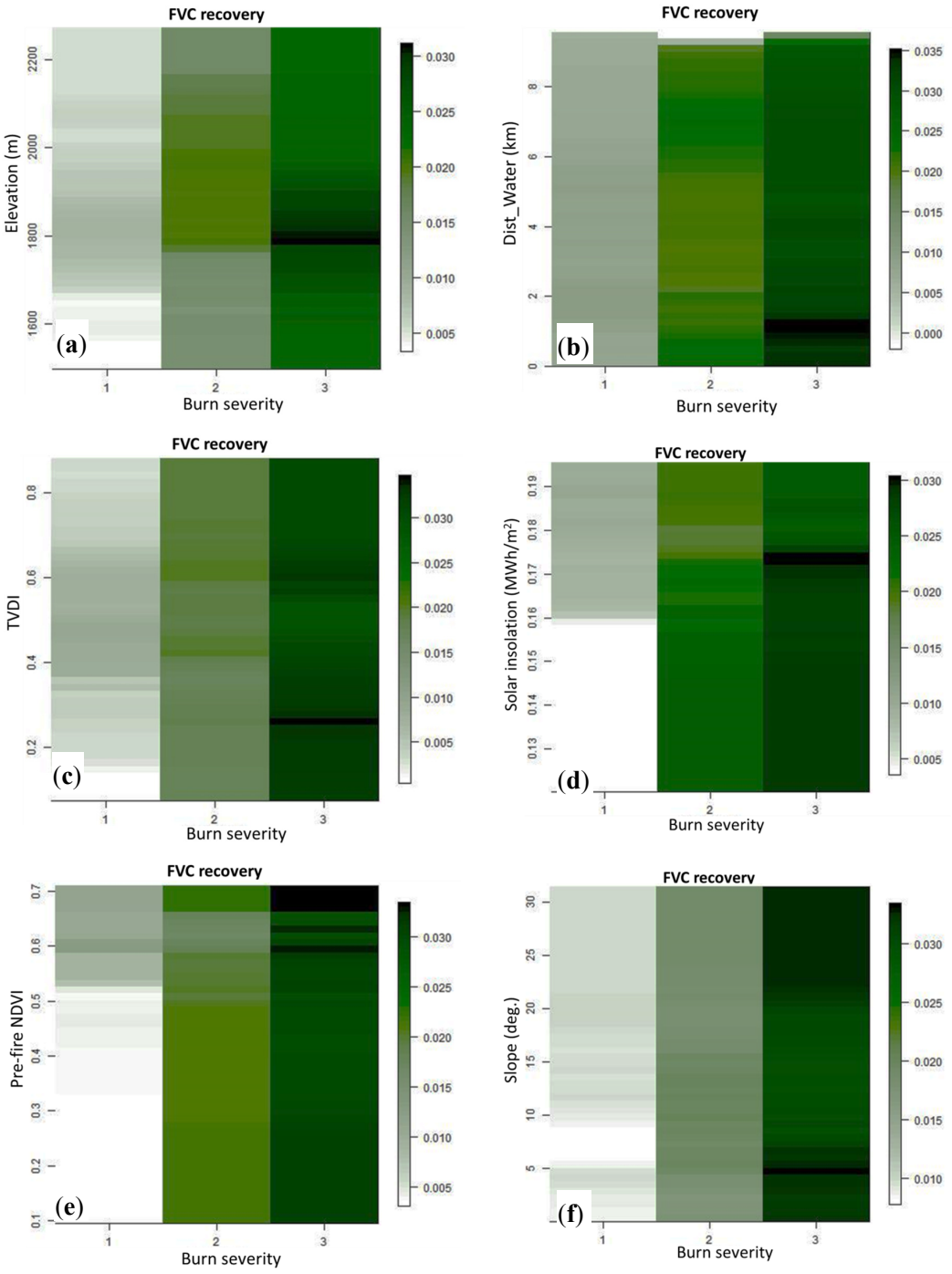

Figure 9. *Cont.*

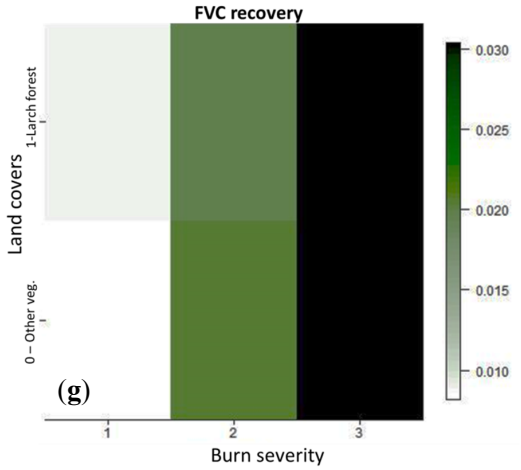

Figure 9. Interaction between burn severity and other environmental factors (**a**: burn severity and elevation; **b**: burn severity and distance to water bodies; **c**: burn severity and temperature - vegetation dryness index (TVDI); **d**: burn severity and solar insolation; **e**: burn severity and pre-fire normalized difference vegetation index (NDVI); **f**: burn severity and slope; **g**: burn severity and pre-fire land covers) in predicting the post-fire vegetation recovery rate defined by FVC. In each interaction plot, the remaining predictor variables were fixed at their mean (for continuous predictors) or their mode (for categorical predictors). Values in the legends show the vegetation recovery rate measured by the FVC slope.

3.2.2. Modeling FRI Based Forest Regeneration

The RF model of FRI-predicted forest recovery indicated that approximately 40% of the variance in post-fire forest recovery can be explained using selected drivers (Table 2). Similar to the FVC based model, the variance explained in each model suggests that there are additional factors (e.g., fire frequency and intensity, soil properties and permafrost condition) that should be included in the models to further explain variation in the post-fire regeneration across the burned area. Validation results from the FRI based model using the independent dataset showed a strong linear relationship between the observed and predicted values of the forest recovery rate (Figure 10a). The rate of post-fire Larch recruitment had the strongest relationship with burn severity, followed by distance to water, pre-fire vegetation condition (i.e., pre-fire NDVI), solar radiation, slope, dryness temperature, cover and elevation (Figure 10b). Compared with FVC based vegetation recovery, elevation was of little importance to determine Larch forest recovery.

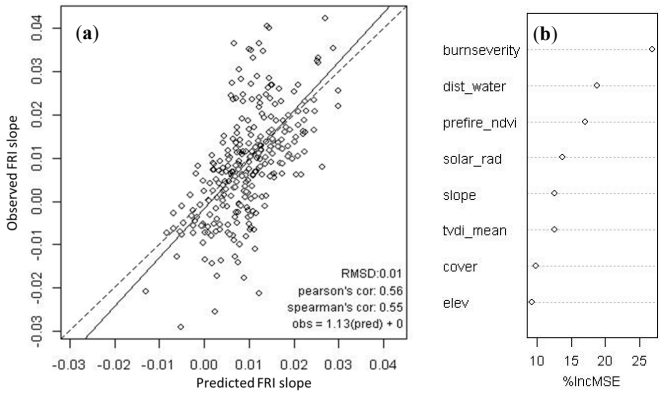

Figure 10. Observed and predicted FRI based forest recovery rate using the random forest algorithm (**a**) and the importance of predictors in classifying forest recovery rates (**b**). The importance of predictions measures the increase of mean square error (MSE) in the classification of a response variable if one of these predictors is excluded from the model.

Interaction plots of FRI model data showed more distinctive patterns in the relationship between the forest recovery rate and predictor variables (Figure 11). Post-fire Larch forest regeneration was strongly related to burn severity in which the highest rate of regeneration was found in the moderate severity areas, followed by the low and high severity burns (Figure 11). The forest regeneration rate was positively correlated with the pre-fire vegetation condition that is defined by the pre-fire NDVI (Figure 11b), photosynthetically active radiation defined by the solar insolation (Figure 11c), slope (Figure 11d), and soil moisture (Figure 11e). However, the forest regeneration rate was inversely correlated with the distance to water (Figure 11a) at all burn severity classes. The highest rate of forest recruitment was found in the Larch burned areas that were close (<3 km) to water, had healthy (NDVI > 0.55) pre-fire vegetation condition and high soil moisture (TVDI < 0.2). In addition to the burn severity factor, these results suggest the importance of microclimate, seed availability and soil water content within the burned area that can accelerate the regeneration of the Larch forest.

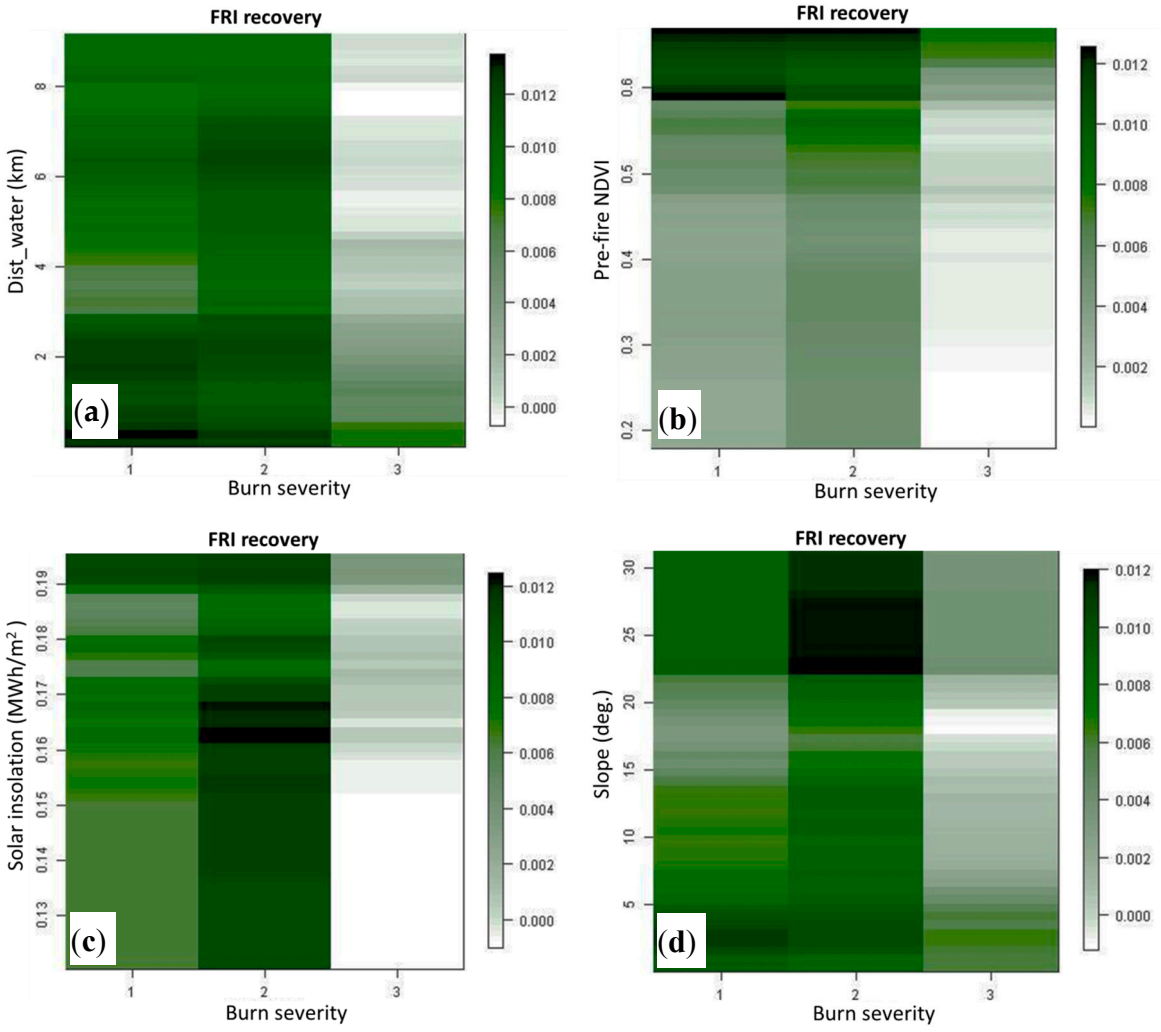

Figure 11. *Cont.*

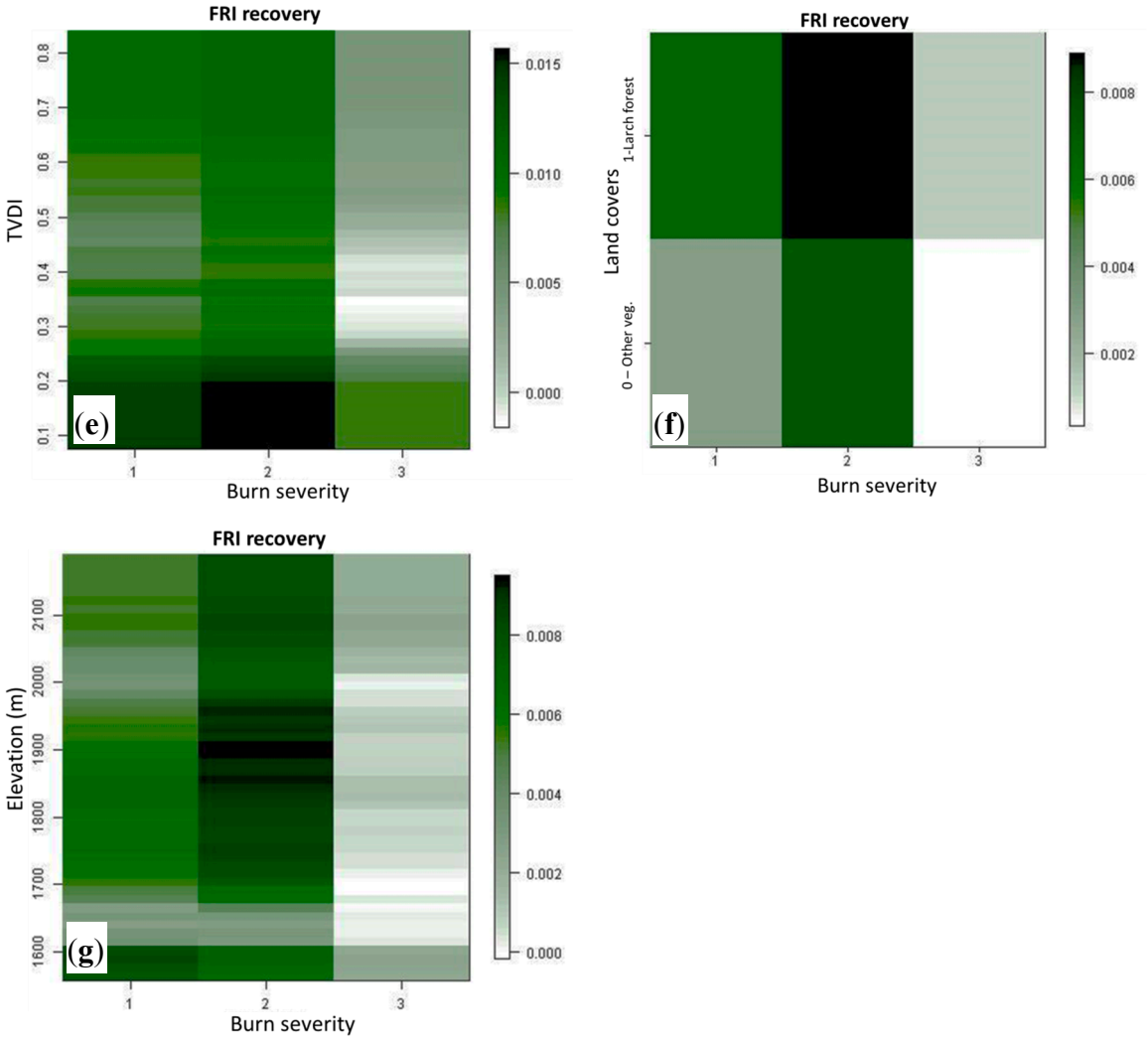

Figure 11. Interaction between burn severity and other factors (**a**: burn severity and distance to water bodies; **b**: burn severity and pre-fire normalized difference vegetation index (NDVI); **c**: burn severity and solar insolation; **d**: burn severity and slope; **e**: burn severity and temperature - vegetation dryness index (TVDI); **f**: burn severity and pre-fire land covers; **g**: burn severity and elevation) in predicting post-fire forest recovery pattern defined by FRI. In each interaction plot, the unplotted predictor variables were fixed at their mean (for continuous predictors) or their mode (for categorical predictors). Values in the legends show the forest recovery rate measured by FRI slope.

4. Discussion

4.1. Influence of Burn Severity on Post-Fire Vegetation Response

In both FVC and FRI models, variables generally ranked similarly between the two models. Burn severity was by far the most important driver in determining patterns of the forest recovery. This finding is consistent with other studies in boreal regions [8,49] that indicate the primary control of burn severity on post-fire succession. However, our results reveal that the influence of burn severity on the early stages of forest succession is different when measuring Larch recruitment itself. Specifically, higher burn severity resulted in a higher rate of green vegetation recovery as predicted by FVC, while the moderate burn severity was the most favorable condition for Larch tree recruitment in later stages as defined by the FRI. These findings are similar to other remote sensing based studies. Epting and Verbyla [80] found that post-fire NDVI based green vegetation recovery in the Alaskan

boreal forest is fastest in high burn severity locations, followed by moderate and low burn severity areas. Similarly, Jin et al. [81] used the MODIS enhanced vegetation index (EVI) as an indicator of the post-fire vegetation recovery in the North American boreal forests and found that more severe fires lead to more rapid post-fire EVI increases. According to Johnstone et al. [82], the higher consumption of organic layers in severe fires results in more mineral soil exposure that favors growth of herbaceous species and broadleaf trees. These shade-intolerant species often grow quickly in early stages of post-fire forest succession [25,83,84] and respond positively to increased burn severity [45,49,84]. As a result, vegetation indices such as the NDVI, EVI, and NDVI based FVC which are sensitive to the changes of green vegetation canopy several years after the fire [81,85] are positively correlated with burn severity.

Our remote sensing based estimates of the Larch forest recovery rate in later successional stages ($\geq$10 years since fire) found that the moderate burn severity sites recovered faster, followed by low and high severity sites (Figure 11). This pattern of Larch regeneration with respect to burn severity is consistent with our field-based assessment conducted 13-years post-fire. We found that moderate burn severity was the most suitable condition for Larch forest regeneration with the highest density of 16×10^3 saplings/ha, followed by low and high burn severity sites with 740 saplings/ha and 630 saplings/ha, respectively (see Table 2, [23]). Even though seed and seedling density was highest (92×10^4 seeds/ha and 4.86×10^4 seedlings/ha) in the low severity sites, these seeds and seedlings could hardly grow to become saplings due to competition from the high density of undamaged parent trees (526 trees/ha) that resulted in low light availability for photosynthesis in the understory of low severity sites [28]. Compared with low and moderate burn severity sites, seed density in high severity burns was very low due to both the limitation of seed dispersal from the very few remaining adult trees (<42 trees/ha) and high seed death in severe fires. Consequently, moderate burn severity sites with a high seed density (40×10^4 seeds/ha) and light availability due to the low to moderate density of unburned parent trees (101 trees/ha) seem to create favorable conditions for seed germination and sapling growth compared with the high and low severity burned forest.

The relationship between burn severity and Larch regeneration in our study differs from studies in the Alaska interior boreal Black Spruce forest where the burn severity is positively correlated with seedling establishment [82] and in the northeast China boreal Larch forest where the density of tree recruitment (both conifer and broadleaf trees) is negatively correlated with burn severity [8]. These differences are likely confounded by several factors such as the experiment design, fire ecology, soil organic layer depth and the regeneration ecology of the dominant tree species. Cai et al. [8] only used two burn severity classes (low and high) and included both seedling and sapling density in post-fire tree recruitment density. If both seedlings and saplings had been included in our field-based and remotely-sensed study, we would have found a similar, negative relationship between post-fire tree-recruitment and burn severity as shown in Cai et al.'s study. Remotely sensed observation is often highly correlated with overstory properties. Distinguishing between seedling and sapling density is thus necessary to be able to capture overstory forest using remote sensing. It should also be noted that, from our field observations, seedling-to-sapling growth in low burn severity sites was negligible. This was possibly due to competition from the high density of remaining, parent trees.

North American boreal conifers survive in crown-fire dominated ecosystems by storing seeds in serotinous cones that can disperse seeds after a fire and are thus able to regenerate as a shade tolerant species growing in an understory of pioneer species [86]. In our study area, increased burn severity dramatically decreases Larch seeds available for regeneration (92×10^4 seeds/ha in low severity sites and 4×10^4 seeds/ha in high severity sites). The lack of seeds in high burn severity sites can thus constrain post-fire Larch recruitment. However, as discussed previously, our finding of green vegetation recovery in early successional forests as measured by FVC is consistent with North American studies. These results suggest that variation in forest recovery related to burn severity is a general property of deciduous conifer and broadleaf boreal forests.

4.2. Influence of Other Environmental Factors on Post-Fire Vegetation Response

Even though burn severity has been found to be an important factor influencing post-fire forest patterns ([6,8,49,81,82,84], this study), many other environmental factors likely affect the recovery of post-fire vegetation. In this study, we investigated the influence of other factors related to the site conditions on variation of post-fire forest recovery. Our results showed that soil and air water content, defined by the distance to a water body and TVDI variables, is likely the second most important driver of recovery in both early and late recovering species following fire disturbances. In particular, Larch forest regeneration clearly had a positive relationship with water content (Figure 11a,e). The results of our field observations showed that a much higher number of saplings was found in plots closer to a lake. This suggests the importance of water balance for Larch growth. This finding is similar to the studies in the North American boreal forest in which the dramatically lower levels of tree recruitment (both broadleaf and conifer) were found in sites with lower soil moisture [51,82]. For the long-term Larch forest growth, changes in water-related factors such as temperature, precipitation, soil moisture and water potential due to climate change are important factors for influencing Larch forest growth and regeneration [1,4,11,87]. For example, young Larch trees growing in the taiga-steppe forest are more susceptible to drought than mature trees at the same sites [87]. Similarly, recent declines of Larch forests at the southern limit of the Siberian boreal forest are attributed to decreasing effective moisture due to increasing summer temperature and decreasing summer precipitation as a result of climate change [1,11].

Our results showed that elevation was the least important variable in predicting the regeneration rate of the Larch forest while it was the second most important variable for explaining patterns of green vegetation cover. This suggests that the rate of green vegetation recovery is more varied across elevations than it generally is in Larch dominated regrowth. Even though our field observations and other studies [8,82] showed that conifer recruitment in boreal forests is negatively correlated with the elevation, other factors related to burn severity, soil water content, pre-fire vegetation condition and solar insolation are the most important variables to predict forest regeneration [2,8,27]. These results suggest that such factors obscure elevation factor as a predictive variable for determining Larch regeneration in our ecosystem.

Solar insolation was also an important factor that showed a positive correlation with the green vegetation recovery rate at low burn severity (Figure 9d) and the Larch regeneration rate (Figure 11c). Nevertheless, it was negatively correlated with the green vegetation recovery rate at moderate and high burn severity (Figure 9d). Solar insolation is not only related to soil temperature and moisture [63] but also has a linear relationship with photosynthetically active radiation [65]. Negative or positive responses of both green vegetation and Larch dominated regrowth to total summer solar insolation depended on burn severity in our study. This reflects the basic photosynthetic need for light for post-fire vegetation to regrow. In the early stages of post-fire forest succession, low burn severity sites are still dominated by undamaged adult trees. Therefore, an increase in solar insolation in low burn severity sites is necessary for light penetration through the closed, overstory canopy. This promotes photosynthetic activity for the growth of vegetation in understory canopies or tree-fall gaps. This might also be a reason for the positive Larch regeneration response in later successional stages as indicated by the FRI (Figure 11c). Here, regenerated saplings are still partially or completely covered by overstory canopies of both shade intolerant species and remaining adult trees. However, it is worth mentioning that the ability of understory trees to grow and survive in shade is the outcome of complex interactions between leaf- and plant-level responses to light, nutrients, and water availability [88,89]. In the cases of a negative response to solar insolation of early successional stages in moderate and high burn severity sites (Figure 9c), an increase of leaf temperature under high solar insolation that leads to decrease of the net photosynthetic rate may be influential [90].

Both green vegetation and Larch dominated recovery stages of the post-fire forest were positively correlated with pre-fire forest condition (Figures 9e and 11b). The importance of pre-fire NDVI, particularly in predicting Larch regeneration, may be related to the basal area of the pre-fire Larch

forest. Seed production and seedling densities have been shown to be positively correlated with pre-fire basal areas [3,82,91,92]. Higher pre-fire NDVI thus results in higher seed productivity that can promote post-fire regeneration. A high recruitment rate of shade-intolerant species such as grass, shrub and herbaceous plants in early successional stages after a fire was also expected in the areas with higher pre-fire NDVI, as they can provide a bank of roots and stumps for asexual recovery of these species. Similarly, the higher forest regeneration rate in the Larch burned areas not only suggests the importance of seed availability but also microclimate conditions and soil properties in the post-fire Larch environment for seed germination and growth.

Even though we evaluated multiple factors related to fire and environmental conditions that affect the patterns of post-fire forest succession in the boreal Larch forest, these factors only accounted for 40%–50% of the variance in forest recovery explained by the models. Many other unstudied parameters might also have strong direct- or indirect-influences on post-fire biotic patterns. In addition to burn severity, other parameters of the fire behavior such as fire intensity, fire severity and fire frequency are significant factors in determining the heterogeneity of post-fire landscape including species composition [2,25,27,93,94]. For example, high and very high fire frequency may lead to replacement of forest vegetation by nonarboreal vegetation such as meadow, shrub, or tundra, and many even take 50 to hundreds of years to recover to the pre-fire condition [25,95]. Fire intensity and initial fire severity may be important variables that may be more highly correlated with vegetation recovery than the burn severity predictor variable.

Unfortunately, estimates of fire intensity and fire severity (i.e., an initial and early assessment after fire activity [47,96]) by remote sensing were not feasible in this study as they require satellite images acquired during or shortly after the fire event. Nevertheless, it should be noted that measured burn severity is already an extended assessment using remotely sensed measures as surrogates of fire intensity and severity in monitoring the post-fire effects [7,96–98].

Additionally, post-fire soil properties, soil organic layer depth and permafrost conditions are factors that can drive patterns of boreal forest recovery. Kasischke et al. [51] found that organic layer depth remaining after fire is positively correlated with post-fire conifer seedling density, while it negatively affected the broadleaf recruitment and growth in the North American boreal forest. These patterns of tree recruitment in post-fire boreal forests are further affected by soil moisture [51], soil burn severity, pre-fire conifer and broadleaf basal area and drainage [45]. Siberian boreal Larch forests typically have a pre-fire organic layer much thinner than the North American boreal forest, about 10 cm and 25 cm respectively [8,99]. Organic layer depth significantly affects the depth of soil thawing that, in turn, can drive Larch forest growth and regeneration [99]. In addition to differences in fire types and species characteristics [86], the response of post-fire vegetation with respect to organic layer depth as well as soil thawing depth is expected to differ between these two boreal ecoregions. This requires further investigation.

Finally, even though the RF algorithm is non-parametric and might be unaffected by the distributional assumptions as well as spatial autocorrelation [71,73,100], further analysis in the influence of these assumptions on the results of this study is still necessary to quantify the uncertainties of the derived models. For example, Kane et al. [101] found that there were differences in variance explained by predictor variables if the RF models were developed with different sample distances. Kane et al. also mentioned that the closer sampling (e.g., 45–180 m) can be used to catch fine scale heterogeneity of ecological conditions as well as to understand the key variations in the biophysical patterns within the study area. On the other hand, the larger sampling distance (e.g., 360–720 m) may provide coarser resolution of biophysical patterns. This idea has potential for future research to understand local and global patterns of post-fire forest recovery based on the analysis of spatial autocorrelation in predictor variables.

4.3. Implications for Post-Fire Forest Succession and Forest Management

Post-fire successional trajectories in Larch forests are highly sensitive to variation in fire regimes, the physical environment and species characteristics. With the sensitivity of FVC and FRI to differentiate stages of post-fire forest recovery, an assessment of those driving factors that influence change in FVC and FRI based forest recovery rates has demonstrated consistency with the field-based studies. Even though monitoring of all successional stages after disturbance requires an effort over a long period and/or measures of many biotic and abiotic factors in the post-fire environment, initial forest conditions and tree recruitment immediately (e.g., $\leq$15 years) after a fire can provide a critical observational window to predict canopy patterns and stand dynamics [102]. Therefore, the use of prediction models of an early successional stage and the later stages of sapling and young Larch regrowth based on our selected predictor variables can be useful to identify other successional stages such as the young-to-mature Larch forest succession. For example, a high density of Larch saplings coupled with its high recovery rate measured by the FRI slope in moderate burn severity sites for the first 20 years after fire can be a surrogate of the "self-replacement" succession in these sites. On the other hand, the low recovery rate and lack of seed source for Larch regeneration in high burn severity sites can shift Larch dominated forest to a broadleaf dominated forest.

Variation in the initial stages of post-fire tree recruitment at varying burn severity could result in large, long-term negative impacts on forest carbon storage [103,104]. As shown in this study, the Larch forest in areas of severe burns will require a longer recovery period—or the Larch forest will possibly not recover—to attain the pre-fire level of net primary productivity. This, in turn, will exacerbate climate change and thus fire disturbance effects. Additionally, the transformation of closed forest to open forest or even grassland caused by fires could result in the alteration of other natural, hydrological and biogeochemical cycles [105–107]. Therefore, our study suggests that incorporating fire and environmental factors into how environmental conditions are classified for management purposes would improve our ability to guide restoration towards a desired fire behavior, forest composition, structure and landscape patterns. Landscapes could be evaluated to identify where existing forest communities depart significantly from those expected and thus propose priority areas for silvicultural treatments. We note, however, that our results should be examined in relation to similar burned areas in the same ecoregion to predict comprehensively the behavior of fires and forest responses at regional scales.

5. Conclusions

The influence of fire behavior and environmental factors on the spatiotemporal patterns of Larch forest recruitment and green vegetation recovery as defined by FRI and FVC, respectively, was evaluated in this study using Landsat time-series data. Burn severity was the most important factor explaining the pattern of green vegetation recovery as well as the rate of Larch recruitment. The highest rate of Larch regeneration was found in the sites of moderate burn severity, while a more severe burn was preferable condition for early seral communities of shrubs, grasses, conifers and broadleaf trees to recover. Other factors such as distance to water, pre-fire vegetation condition, solar radiation, slope, dryness temperature also play important roles in determining the regeneration of dominant Larch trees in the post-fire Siberian forest. Further studies are necessary to ascertain a greater understanding of the uncertainty surrounding the random forest based models of post-fire forest patterns in this study.

Acknowledgments: The authors would like to acknowledge the financial support of the Vietnamese International Education Development scholarship, the Department of Geography and Planning at the University of Saskatchewan, and the Grant in Aid for Scientific Research No. 22405022 from the Ministry of Education, Science, Sports and Culture, Japan.

Author Contributions: Thuan Chu carried out most of the image processing and drafted the manuscript text. Xulin Guo supervised the steps of data collecting and processing. The field data for the validation and discussion of the results were provided by Kazuo Takeda. Both co-authors also provided comments and revised the manuscript.

Conflicts of Interest: The authors declare no conflict of interest.

References

1. Dulamsuren, C.; Hauck, M.; Khishigjargal, M.; Leuschner, H.H.; Leuschner, C. Diverging climate trends in mongolian taiga forests influence growth and regeneration of larix sibirica. *Oecologia* **2010**, *163*, 1091–1102. [CrossRef] [PubMed]
2. Otoda, T.; Doi, T.; Sakamoto, K.; Hirobe, M.; Nachin, B.; Yoshikawa, K. Frequent fires may alter the future composition of the boreal forest in northern Mongolia. *J. For. Res.* **2013**, *18*, 246–255. [CrossRef]
3. James, T.M. Temperature sensitivity and recruitment dynamics of siberian larch (larix sibirica) and siberian spruce (picea obovata) in northern Mongolia's boreal forest. *For. Ecol. Manag.* **2011**, *262*, 629–636. [CrossRef]
4. Dulamsuren, C.; Hauck, M.; Leuschner, C. Recent drought stress leads to growth reductions in larix sibirica in the western khentey, mongolia. *Glob. Chang. Biol.* **2010**, *16*, 3024–3035. [CrossRef]
5. Barrett, K.; McGuire, A.; Hoy, E.; Kasischke, E. Potential shifts in dominant forest cover in interior alaska driven by variations in fire severity. *Ecol. Appl.* **2011**, *21*, 2380–2396. [CrossRef] [PubMed]
6. Shenoy, A.; Johnstone, J.F.; Kasischke, E.S.; Kielland, K. Persistent effects of fire severity on early successional forests in interior alaska. *For. Ecol. Manag.* **2011**, *261*, 381–390. [CrossRef]
7. French, N.H.F.; Kasischke, E.S.; Hall, R.J.; Murphy, K.A.; Verbyla, D.L.; Hoy, E.E.; Allen, J.L. Using landsat data to assess fire and burn severity in the north American boreal forest region: An overview and summary of results. *Int. J. Wildland Fire* **2008**, *17*, 443–462. [CrossRef]
8. Cai, W.; Yang, J.; Liu, Z.; Hu, Y.; Weisberg, P.J. Post-fire tree recruitment of a boreal larch forest in northeast China. *For. Ecol. Manag.* **2013**, *307*, 20–29. [CrossRef]
9. Johnstone, J.; Chapin, F., III. Fire interval effects on successional trajectory in boreal forests of northwest Canada. *Ecosystems* **2006**, *9*, 268–277. [CrossRef]
10. Veilleux-Nolin, M.; Payette, S. Influence of recent fire season and severity on black spruce regeneration in spruce–moss forests of Quebec, Canada. *Can. J. For. Res.* **2012**, *42*, 1316–1327. [CrossRef]
11. Dulamsuren, C.; Wommelsdorf, T.; Zhao, F.; Xue, Y.; Zhumadilov, B.Z.; Leuschner, C.; Hauck, M. Increased summer temperatures reduce the growth and regeneration of larix sibirica in southern boreal forests of eastern Kazakhstan. *Ecosystems* **2013**, *16*, 1536–1549. [CrossRef]
12. Chu, T.; Guo, X. Remote sensing techniques in monitoring post-fire effects and patterns of forest recovery in boreal forest regions: A review. *Remote Sens.* **2013**, *6*, 470–520. [CrossRef]
13. Ireland, G.; Petropoulos, G.P. Exploring the relationships between post-fire vegetation regeneration dynamics, topography and burn severity: A case study from the montane cordillera ecozones of western Canada. *Appl. Geogr.* **2015**, *56*, 232–248. [CrossRef]
14. Petropoulos, G.P.; Griffiths, H.M.; Kalivas, D.P. Quantifying spatial and temporal vegetation recovery dynamics following a wildfire event in a Mediterranean landscape using Eo data and GIS. *Appl. Geogr.* **2014**, *50*, 120–131. [CrossRef]
15. Malak, D.A.; Pausas, J.G.; Pardo-Pascual, J.E.; Ruiz, L.A. Fire recurrence and the dynamics of the enhanced vegetation index in a Mediterranean ecosystem. *Int. J. Appl. Geospat. Res.* **2015**, *6*, 18–35. [CrossRef]
16. Frolking, S.; Palace, M.; Clark, D.; Chambers, J.; Shugart, H.; Hurtt, G. Forest disturbance and recovery: A general review in the context of spaceborne remote sensing of impacts on aboveground biomass and canopy structure. *J. Geophys. Res.* **2009**, *114*, G00E02. [CrossRef]
17. Buma, B. Evaluating the utility and seasonality of ndvi values for assessing post-disturbance recovery in a subalpine forest. *Environ. Monit. Assess.* **2012**, *184*, 3849–3860. [CrossRef] [PubMed]
18. Fernandez-Manso, A.; Quintano, C.; Roberts, D.A. Burn severity influence on post-fire vegetation cover resilience from landsat mesma fraction images time series in Mediterranean forest ecosystems. *Remote Sens. Environ.* **2016**, *184*, 112–123. [CrossRef]
19. Gitelson, A.A.; Kaufman, Y.J.; Stark, R.; Rundquist, D. Novel algorithms for remote estimation of vegetation fraction. *Remote Sens. Environ.* **2002**, *80*, 76–87. [CrossRef]
20. Vila, J.P.S.; Barbosa, P. Post-fire vegetation regrowth detection in the deiva marina region (liguria-italy) using landsat tm and etm+ data. *Ecol. Model.* **2010**, *221*, 75–84. [CrossRef]
21. Huang, C.; Song, K.; Kim, S.; Townshend, J.R.; Davis, P.; Masek, J.G.; Goward, S.N. Use of a dark object concept and support vector machines to automate forest cover change analysis. *Remote Sens. Environ.* **2008**, *112*, 970–985. [CrossRef]

22. Huang, C.; Goward, S.N.; Schleeweis, K.; Thomas, N.; Masek, J.G.; Zhu, Z. Dynamics of national forests assessed using the landsat record: Case studies in eastern united states. *Remote Sens. Environ.* **2009**, *113*, 1430–1442. [CrossRef]
23. Chu, T.; Guo, X.; Takeda, K. Remote sensing approach to detect post-fire vegetation regrowth in siberian boreal larch forest. *Ecol. Indic.* **2016**, *62*, 32–46. [CrossRef]
24. Tsogtbaatar, J. Deforestation and reforestation needs in mongolia. *For. Ecol. Manag.* **2004**, *201*, 57–63. [CrossRef]
25. Zyryanova, O.; Abaimov, A.; Bugaenko, T.; Bugaenko, N. Recovery of forest vegetation after fire disturbance. In *Permafrost Ecosystems*; Springer: Berlin/Heidelberg, Germany, 2010; pp. 83–96.
26. Farukh, M.A.; Hayasaka, H.; Mishigdorj, O. Recent tendency of mongolian wildland fire incidence: Analysis using modis hotspot and weather data. *J. Nat. Disaster Sci.* **2009**, *31*, 23–33. [CrossRef]
27. International Forest Fire News. The forest fire situation in mongolia. *Int. For. Fire News* **2007**, *36*, 46–66.
28. Takeda, K.; Torita, H.; Nobori, Y.; Lopez, C.M.L.; Itoh, J. Regeneration in burned larch forests of hovsgol region, northern Mongolia. In *Multidisciplinary Research on Mongolian Ecosystems: Conference Proceedings from Second International Symposium by Japan and Mongolia*; Japan Society of Forest Planning Press: Niigata, Japan, 2013.
29. Chu, T.; Guo, X.; Takeda, K. Temporal dependence of burn severity assessment in siberian larch (*larix sibirica*) forest of northern Mongolia using remotely sensed data. *Int. J. Wildland Fire* **2016**, *25*, 685–698. [CrossRef]
30. USGS Global Visualization Viewer. Avalable online: http://glovis.usgs.gov/ (accessed on 15 May 2013).
31. Schroeder, T.A.; Cohen, W.B.; Song, C.; Canty, M.J.; Yang, Z. Radiometric correction of multi-temporal landsat data for characterization of early successional forest patterns in western Oregon. *Remote Sens. Environ.* **2006**, *103*, 16–26. [CrossRef]
32. Canty, M.J.; Nielsen, A.A. Automatic radiometric normalization of multitemporal satellite imagery with the iteratively re-weighted mad transformation. *Remote Sens. Environ.* **2008**, *112*, 1025–1036. [CrossRef]
33. Richter, R. A fast atmospheric correction algorithm applied to landsat tm images. *Int. J. Remote Sens.* **1990**, *11*, 159–166. [CrossRef]
34. SRTM. Avalable online: http://earthexplorer.usgs.gov/ (accessed on 30 April 2014).
35. Carlson, T.N.; Ripley, D.A. On the relation between ndvi, fractional vegetation cover, and leaf area index. *Remote Sens. Environ.* **1997**, *62*, 241–252. [CrossRef]
36. Wittich, K.; Hansing, O. Area-averaged vegetative cover fraction estimated from satellite data. *Int. J. Biometeorol.* **1995**, *38*, 209–215. [CrossRef]
37. Yang, G.; Pu, R.; Zhang, J.; Zhao, C.; Feng, H.; Wang, J. Remote sensing of seasonal variability of fractional vegetation cover and its object-based spatial pattern analysis over mountain areas. *ISPRS J. Photogramm. Remote Sens.* **2013**, *77*, 79–93. [CrossRef]
38. Tucker, C.J. Red and photographic infrared linear combinations for monitoring vegetation. *Remote Sens. Environ.* **1979**, *8*, 127–150. [CrossRef]
39. Keeley, J.E.; Keeley, M.B.; Bond, W.J. Stem demography and post-fire recruitment of a resprouting serotinous conifer. *J. Veg. Sci.* **1999**, *10*, 69–76. [CrossRef]
40. Turner, M.G.; Romme, W.H.; Gardner, R.H. Prefire heterogeneity, fire severity, and early postfire plant reestablishment in subalpine forests of yellowstone national park, wyoming. *Int. J. Wildland Fire* **1999**, *9*, 21–36. [CrossRef]
41. Pausas, J.; Ribeiro, E.; Vallejo, R. Post-fire regeneration variability of pinus halepensis in the eastern Iberian Peninsula. *For. Ecol. Manag.* **2004**, *203*, 251–259. [CrossRef]
42. Shive, K.L.; Kuenzi, A.M.; Sieg, C.H.; Fulé, P.Z. Pre-fire fuel reduction treatments influence plant communities and exotic species 9 years after a large wildfire. *Appl. Veg. Sci.* **2013**, *16*, 457–469. [CrossRef]
43. Lee, J.-M.; Lee, S.-W.; Lim, J.-H.; Won, M.-S.; Lee, H.-S. Effects of heterogeneity of pre-fire forests and vegetation burn severity on short-term post-fire vegetation density and regeneration in Samcheok, Korea. *Landsc. Ecol. Eng.* **2014**, *10*, 215–228. [CrossRef]
44. Lozano, F.J.; Suárez-Seoane, S.; de Luis-Calabuig, E. Does fire regime affect both temporal patterns and drivers of vegetation recovery in a resilient Mediterranean landscape? A remote sensing approach at two observation levels. *Int. J. Wildland Fire* **2012**, *21*, 666–679. [CrossRef]
45. Johnstone, J.F.; Kasischke, E.S. Stand-level effects of soil burn severity on postfire regeneration in a recently burned black spruce forest. *Can. J. For. Res.* **2005**, *35*, 2151–2163. [CrossRef]

46. Pettorelli, N.; Vik, J.O.; Mysterud, A.; Gaillard, J.-M.; Tucker, C.J.; Stenseth, N.C. Using the satellite-derived ndvi to assess ecological responses to environmental change. *Trends Ecol. Evol.* **2005**, *20*, 503–510. [CrossRef] [PubMed]
47. Lentile, L.B.; Holden, Z.A.; Smith, A.M.S.; Falkowski, M.J.; Hudak, A.T.; Morgan, P.; Lewis, S.A.; Gessler, P.E.; Benson, N.C. Remote sensing techniques to assess active fire characteristics and post-fire effects. *Int. J. Wildland Fire* **2006**, *15*, 319–345. [CrossRef]
48. Key, C.H.; Benson, N.C. *Landscape Assessment: Ground Measure of Severity, the Composite Burn Index; and Remote Sensing of Severity, the Normalized Burn Ratio*; Lutes, D.C., Keane, R.E., Caratti, J.F., Key, C.H., Benson, N.C., Sutherland, S., Gangi, L.J., Eds.; General Techincal Report RMRS-GTR-164-CD: LA; USDA Forest Service, Rocky Mountain Research Station: Ogden, UT, USA, 2006; pp. 1–15.
49. Johnstone, J.F.; Chapin, F.S., III. Effects of soil burn severity on post-fire tree recruitment in boreal forest. *Ecosystems* **2006**, *9*, 14–31. [CrossRef]
50. Kasischke, E.S.; Johnstone, J.F. Variation in postfire organic layer thickness in a black spruce forest complex in interior alaska and its effects on soil temperature and moisture. *Can. J. For. Res.* **2005**, *35*, 2164–2177. [CrossRef]
51. Kasischke, E.S.; Bourgeau-Chavez, L.L.; Johnstone, J.F. Assessing spatial and temporal variations in surface soil moisture in fire-disturbed black spruce forests in interior alaska using spaceborne synthetic aperture radar imagery—Implications for post-fire tree recruitment. *Remote Sens. Environ.* **2007**, *108*, 42–58. [CrossRef]
52. Sandholt, I.; Rasmussen, K.; Andersen, J. A simple interpretation of the surface temperature/vegetation index space for assessment of surface moisture status. *Remote Sens. Environ.* **2002**, *79*, 213–224. [CrossRef]
53. Wang, C.; Qi, S.; Niu, Z.; Wang, J. Evaluating soil moisture status in china using the temperature-vegetation dryness index (tvdi). *Can. J. Remote Sens.* **2004**, *30*, 671–679. [CrossRef]
54. Chen, J.; Wang, C.; Jiang, H.; Mao, L.; Yu, Z. Estimating soil moisture using temperature–vegetation dryness index (tvdi) in the huang-huai-hai (hhh) plain. *Int. J. Remote Sens.* **2011**, *32*, 1165–1177. [CrossRef]
55. Son, N.T.; Chen, C.F.; Chen, C.R.; Chang, L.Y.; Minh, V.Q. Monitoring agricultural drought in the lower mekong basin using modis ndvi and land surface temperature data. *Int. J. Appl. Earth Obs. Geoinf.* **2012**, *18*, 417–427. [CrossRef]
56. Holzman, M.; Rivas, R.; Piccolo, M. Estimating soil moisture and the relationship with crop yield using surface temperature and vegetation index. *Int. J. Appl. Earth Obs. Geoinf.* **2014**, *28*, 181–192. [CrossRef]
57. Patel, N.; Anapashsha, R.; Kumar, S.; Saha, S.; Dadhwal, V. Assessing potential of modis derived temperature/vegetation condition index (tvdi) to infer soil moisture status. *Int. J. Remote Sens.* **2009**, *30*, 23–39. [CrossRef]
58. Petropoulos, G.; Carlson, T.; Wooster, M.; Islam, S. A review of ts/vi remote sensing based methods for the retrieval of land surface energy fluxes and soil surface moisture. *Prog. Phys. Geogr.* **2009**, *33*, 224–250. [CrossRef]
59. Han, Y.; Wang, Y.; Zhao, Y. Estimating soil moisture conditions of the greater changbai mountains by land surface temperature and ndvi. *IEEE Trans. Geosci. Remote Sens.* **2010**, *48*, 2509–2515.
60. Leon, J.R.R.; van Leeuwen, W.J.D.; Casady, G.M. Using modis-ndvi for the modeling of post-wildfire vegetation response as a function of environmental conditions and pre-fire restoration treatments. *Remote Sens.* **2012**, *4*, 598–621. [CrossRef]
61. Chen, D.; Loboda, T.V.; Krylov, A.; Potapov, P.V. Mapping stand age dynamics of the siberian larch forests from recent landsat observations. *Remote Sens. Environ.* **2016**, *187*, 320–331. [CrossRef]
62. Zhao, F.J.; Shu, L.F.; Wang, M.Y.; Liu, B.; Yang, L.J. Influencing factors on early vegetation restoration in burned area of pinus pumila - larch forest. *Acta Ecol. Sin.* **2012**, *32*, 57–61. [CrossRef]
63. Fu, P.; Rich, P.M. A geometric solar radiation model with applications in agriculture and forestry. *Comput. Electron. Agric.* **2002**, *37*, 25–35. [CrossRef]
64. Meek, D.; Hatfield, J.; Howell, T.; Idso, S.; Reginato, R. A generalized relationship between photosynthetically active radiation and solar radiation. *Agron. J.* **1984**, *76*, 939–945. [CrossRef]
65. Yu, X.; Wu, Z.; Jiang, W.; Guo, X. Predicting daily photosynthetically active radiation from global solar radiation in the contiguous united states. *Energy Convers. Manag.* **2015**, *89*, 71–82. [CrossRef]
66. Oikonomakis, N.; Ganatsas, P. Land cover changes and forest succession trends in a site of natura 2000 network (elatia forest), in northern greece. *For. Ecol. Manag.* **2012**, *285*, 153–163. [CrossRef]

67. Keating, K.A.; Gogan, P.J.; Vore, J.M.; Irby, L.R. A simple solar radiation index for wildlife habitat studies. *J. Wildl. Manag.* **2007**, *71*, 1344–1348. [CrossRef]
68. Fu, P.; Rich, P.M. Design and implementation of the solar analyst: An arcview extension for modeling solar radiation at landscape scales. In Proceedings of the 19th Annual ESRI User Conference, San Diego, CA, USA, 26–30 July 1999; pp. 1–33.
69. Fu, B.; Burgher, I. Riparian vegetation ndvi dynamics and its relationship with climate, surface water and groundwater. *J. Arid Environ.* **2015**, *113*, 59–68. [CrossRef]
70. Christopoulou, A.; Fyllas, N.M.; Andriopoulos, P.; Koutsias, N.; Dimitrakopoulos, P.G.; Arianoutsou, M. Post-fire regeneration patterns of pinus nigra in a recently burned area in mount taygetos, southern Greece: The role of unburned forest patches. *For. Ecol. Manag.* **2014**, *327*, 148–156. [CrossRef]
71. Breiman, L. Random forests. *Mach. Learn.* **2001**, *45*, 5–32. [CrossRef]
72. Freeman, E.; Frescino, T.; Freeman, M.E. *Package 'Modelmap'*; R Development Team: Vienna, Austria, 2014.
73. Falkowski, M.J.; Evans, J.S.; Martinuzzi, S.; Gessler, P.E.; Hudak, A.T. Characterizing forest succession with lidar data: An evaluation for the inland northwest, USA. *Remote Sens. Environ.* **2009**, *113*, 946–956. [CrossRef]
74. Freeman, E.A.; Moisen, G.G.; Coulston, J.W.; Wilson, B.T. Random forests and stochastic gradient boosting for predicting tree canopy cover: Comparing tuning processes and model performance. *Can. J. For. Res.* **2015**, *46*, 323–339. [CrossRef]
75. Strobl, C.; Boulesteix, A.-L.; Kneib, T.; Augustin, T.; Zeileis, A. Conditional variable importance for random forests. *BMC Bioinform.* **2008**, *9*, 1–11. [CrossRef] [PubMed]
76. Zuur, A.F.; Ieno, E.N.; Elphick, C.S. A protocol for data exploration to avoid common statistical problems. *Methods Ecol. Evol.* **2010**, *1*, 3–14. [CrossRef]
77. Renard, K.G.; Foster, G.R.; Weesies, G.A.; Porter, J.P. Rusle: Revised universal soil loss equation. *J. Soil Water Conserv.* **1991**, *46*, 30–33.
78. Liu, B.; Nearing, M.; Risse, L. Slope gradient effects on soil loss for steep slopes. *Trans. ASAE* **1994**, *37*, 1835–1840. [CrossRef]
79. Kosmas, C.; Danalatos, N.; Gerontidis, S. The effect of land parameters on vegetation performance and degree of erosion under Mediterranean conditions. *Catena* **2000**, *40*, 3–17. [CrossRef]
80. Epting, J.; Verbyla, D. Landscape-level interactions of prefire vegetation, burn severity, and postfire vegetation over a 16-year period in interior alaska. *Can. J. For. Res.* **2005**, *35*, 1367–1377. [CrossRef]
81. Jin, Y.; Randerson, J.T.; Goetz, S.J.; Beck, P.S.A.; Loranty, M.M.; Goulden, M.L. The influence of burn severity on postfire vegetation recovery and albedo change during early succession in north American boreal forests. *J. Geophys. Res.* **2012**, *117*, G01036. [CrossRef]
82. Johnstone, J.F.; Hollingsworth, T.N.; Chapin, F.S.; Mack, M.C. Changes in fire regime break the legacy lock on successional trajectories in Alaskan boreal forest. *Glob. Chang. Biol.* **2010**, *16*, 1281–1295. [CrossRef]
83. Dorisuren, C. Post-fire successions of the larch forests in Mongolia. In Proceedings of the First International Central Asian Wildland Fire Joint Conference and Consultation, Ulaanbaatar, Mongolia, 2–6 June 2008; p. 24.
84. Crotteau, J.S.; Morgan Varner, J., III; Ritchie, M.W. Post-fire regeneration across a fire severity gradient in the southern Cascades. *For. Ecol. Manag.* **2013**, *287*, 103–112. [CrossRef]
85. Goetz, S.J.; Fiske, G.J.; Bunn, A.G. Using satellite time-series data sets to analyze fire disturbance and forest recovery across Canada. *Remote Sens. Environ.* **2006**, *101*, 352–365. [CrossRef]
86. de Groot, W.J.; Cantin, A.S.; Flannigan, M.D.; Soja, A.J.; Gowman, L.M.; Newbery, A. A comparison of Canadian and Russian boreal forest fire regimes. *For. Ecol. Manag.* **2013**, *294*, 23–34. [CrossRef]
87. Dulamsuren, C.; Hauck, M.; Bader, M.; Osokhjargal, D.; Oyungerel, S.; Nyambayar, S.; Runge, M.; Leuschner, C. Water relations and photosynthetic performance in larix sibirica growing in the forest-steppe ecotone of northern Mongolia. *Tree Physiol.* **2009**, *29*, 99–110. [CrossRef] [PubMed]
88. Messier, C.; Doucet, R.; Ruel, J.-C.; Claveau, Y.; Kelly, C.; Lechowicz, M.J. Functional ecology of advance regeneration in relation to light in boreal forests. *Can. J. For. Res.* **1999**, *29*, 812–823. [CrossRef]
89. Givnish, T.J. Adaptation to sun and shade: A whole-plant perspective. *Funct. Plant Biol.* **1988**, *15*, 63–92. [CrossRef]
90. Koike, T.; Mori, S.; Zyryanova, O.; Kajimoto, T.; Matsuura, Y.; Abaimov, A. Photosynthetic characteristics of trees and shrubs growing on the north-and south-facing slopes in central Siberia. In *Permafrost Ecosystems*; Springer: Berlin/Heidelberg, Germany, 2010; pp. 273–287.

91. Greene, D.; Noel, J.; Bergeron, Y.; Rousseau, M.; Gauthier, S. Recruitment of picea mariana, pinus banksiana, and populus tremuloides across a burn severity gradient following wildfire in the southern boreal forest of Quebec. *Can. J. For. Res.* **2004**, *34*, 1845–1857. [CrossRef]
92. Chen, H.Y.; Vasiliauskas, S.; Kayahara, G.J.; Ilisson, T. Wildfire promotes broadleaves and species mixture in boreal forest. *For. Ecol. Manag.* **2009**, *257*, 343–350. [CrossRef]
93. Zyryanova, O.A.; Yabarov, V.; Tchikhacheva, T.L.; Koike, T.; Makoto, K.; Matsuura, Y.; Satoh, F.; Zyryanova, V. The structure and biodiversity after fire disturbance in larix gmelinii (rupr.) rupr. Forests, northeastern Asia. *Eurasian J For Res* **2007**, *10*, 19–29.
94. Sofronov, M.; Volokitina, A. Wildfire ecology in continuous permafrost zone. In *Permafrost Ecosystems*; Springer: Berlin/Heidelberg, Germany, 2010; pp. 59–82.
95. Bergeron, Y.; Gauthier, S.; Kafka, V.; Lefort, P.; Lesieur, D. Natural fire frequency for the eastern Canadian boreal forest: Consequences for sustainable forestry. *Can. J. For. Res.* **2001**, *31*, 384–391. [CrossRef]
96. Heward, H.; Smith, A.M.; Roy, D.P.; Tinkham, W.T.; Hoffman, C.M.; Morgan, P.; Lannom, K.O. Is burn severity related to fire intensity? Observations from landscape scale remote sensing. *Int. J. Wildland Fire* **2013**, *22*, 910–918. [CrossRef]
97. Veraverbeke, S.; Lhermitte, S.; Verstraeten, W.W.; Goossens, R. The temporal dimension of differenced normalized burn ratio (dnbr) fire/burn severity studies: The case of the large 2007 peloponnese wildfires in greece. *Remote Sens. Environ.* **2010**, *114*, 2548–2563. [CrossRef]
98. Keeley, J.E. Fire intensity, fire severity and burn severity: A brief review and suggested usage. *Int. J. Wildland Fire* **2009**, *18*, 116–126. [CrossRef]
99. Sofronov, M.A.; Volokitina, A.V.; Kajimoto, T.; Uemura, S. The ecological role of moss-lichen cover and thermal amelioration of larch forest ecosystems in the northern part of Siberia. *Eurasian J. For. Res.* **2004**, *7*, 11–19.
100. Cutler, D.R.; Edwards, T.C.; Beard, K.H.; Cutler, A.; Hess, K.T.; Gibson, J.; Lawler, J.J. Random forests for classification in ecology. *Ecology* **2007**, *88*, 2783–2792. [CrossRef] [PubMed]
101. Kane, V.R.; Cansler, C.A.; Povak, N.A.; Kane, J.T.; McGaughey, R.J.; Lutz, J.A.; Churchill, D.J.; North, M.P. Mixed severity fire effects within the rim fire: Relative importance of local climate, fire weather, topography, and forest structure. *For. Ecol. Manag.* **2015**, *358*, 62–79. [CrossRef]
102. Johnstone, J.F.; Chapin, F., III; Foote, J.; Kemmett, S.; Price, K.; Viereck, L. Decadal observations of tree regeneration following fire in boreal forests. *Can. J. For. Res.* **2004**, *34*, 267–273. [CrossRef]
103. Turner, M.G.; Tinker, D.B.; Romme, W.H.; Kashian, D.M.; Litton, C.M. Landscape patterns of sapling density, leaf area, and aboveground net primary production in postfire lodgepole pine forests, yellowstone national park (USA). *Ecosystems* **2004**, *7*, 751–775. [CrossRef]
104. Liu, Z.; Yang, J. Quantifying ecological drivers of ecosystem productivity of the early-successional boreal larix gmelinii forest. *Ecosphere* **2014**, *5*, art84. [CrossRef]
105. Mayor, A.; Bautista, S.; Llovet, J.; Bellot, J. Post-fire hydrological and erosional responses of a Mediterranean landscpe: Seven years of catchment-scale dynamics. *Catena* **2007**, *71*, 68–75. [CrossRef]
106. Woods, S.W.; Balfour, V.N. The effects of soil texture and ash thickness on the post-fire hydrological response from ash-covered soils. *J. Hydrol.* **2010**, *393*, 274–286. [CrossRef]
107. Certini, G. Effects of fire on properties of forest soils: A review. *Oecologia* **2005**, *143*, 1–10. [CrossRef] [PubMed]